Electronic Supplementary Information

Quinoline-tagged fluorescent organic probes for sensing of nitro-phenolic compounds and Zn^{2+} ion at ppb level†

Gouri Chakraborty, Prasenjit Das, and Sanjay K. Mandal*

Department of Chemical Sciences, Indian Institute of Science Education and Research Mohali, Sector 81, Manauli PO, S.A.S. Nagar, Mohali, Punjab 140306, India

*Corresponding Author's E-mail: sanjaymandal@iisermohali.ac.in

Table of Contents

Section-1: Characterization of 1 and 2

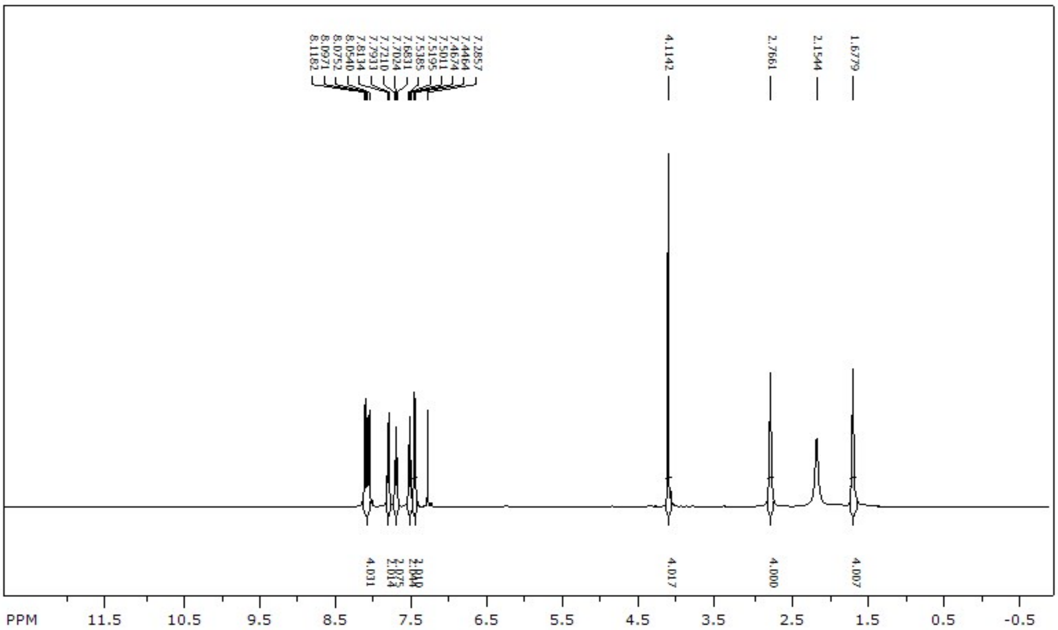

Fig. S1 ^{1}H NMR spectrum of **H_2bqbn** in $CDCl_3$.

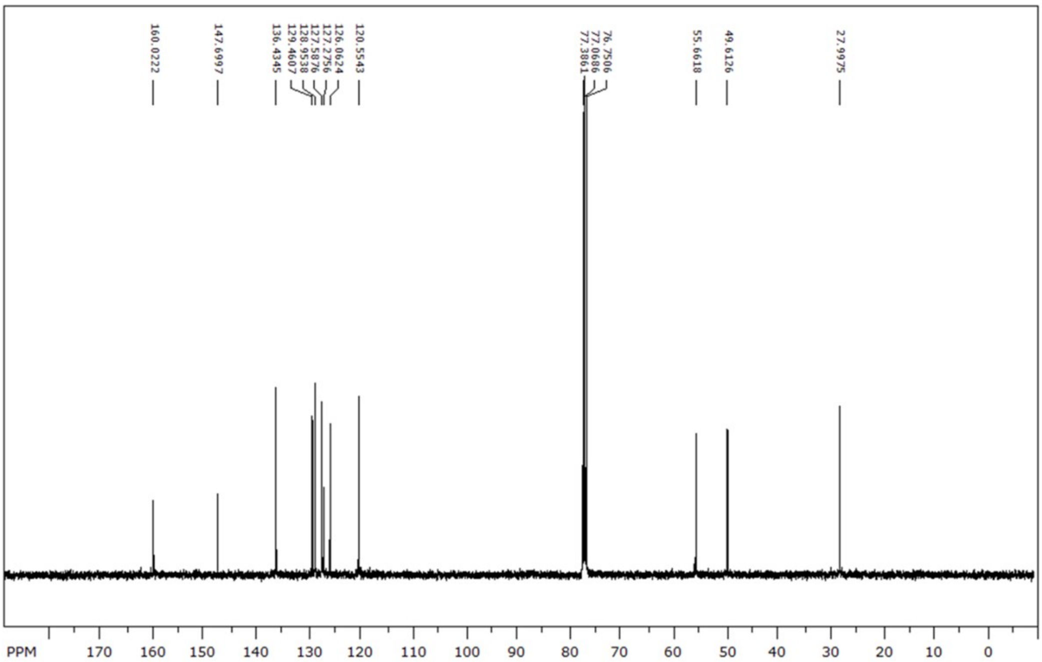

Fig. S2 ^{13}C NMR spectrum of **H_2bqbn** in $CDCl_3$.

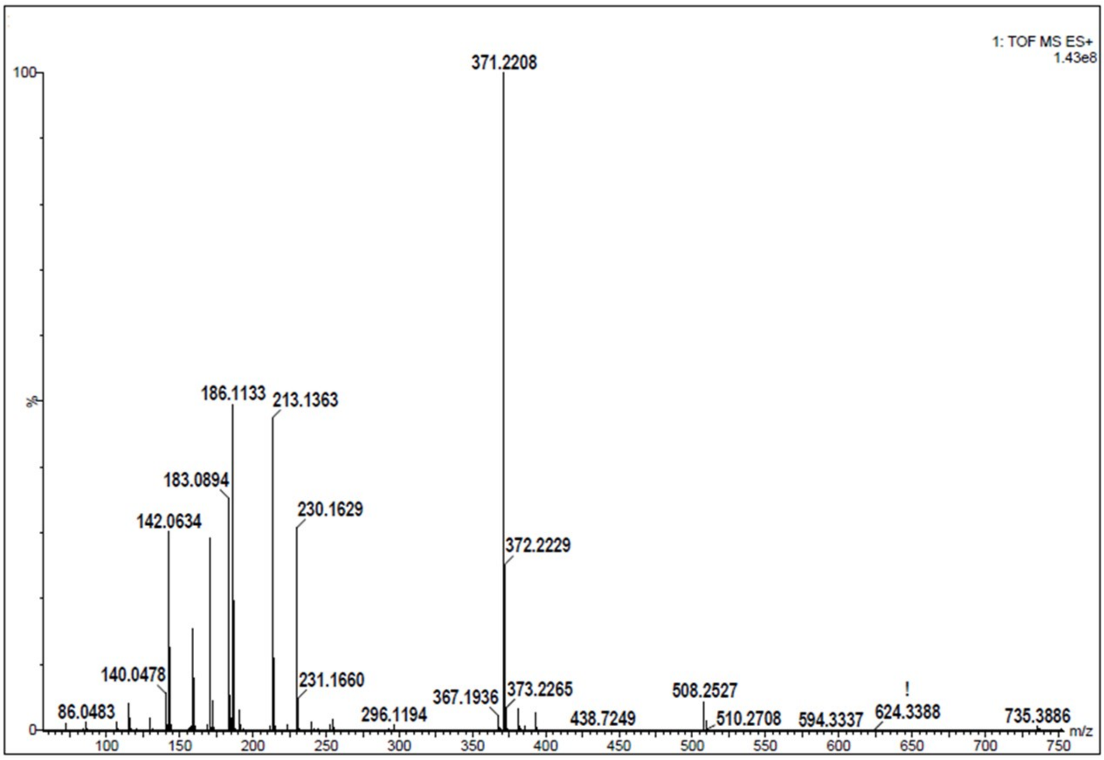

Fig. S3 HRMS spectrum of $\mathbf{H_2bqbn}$.

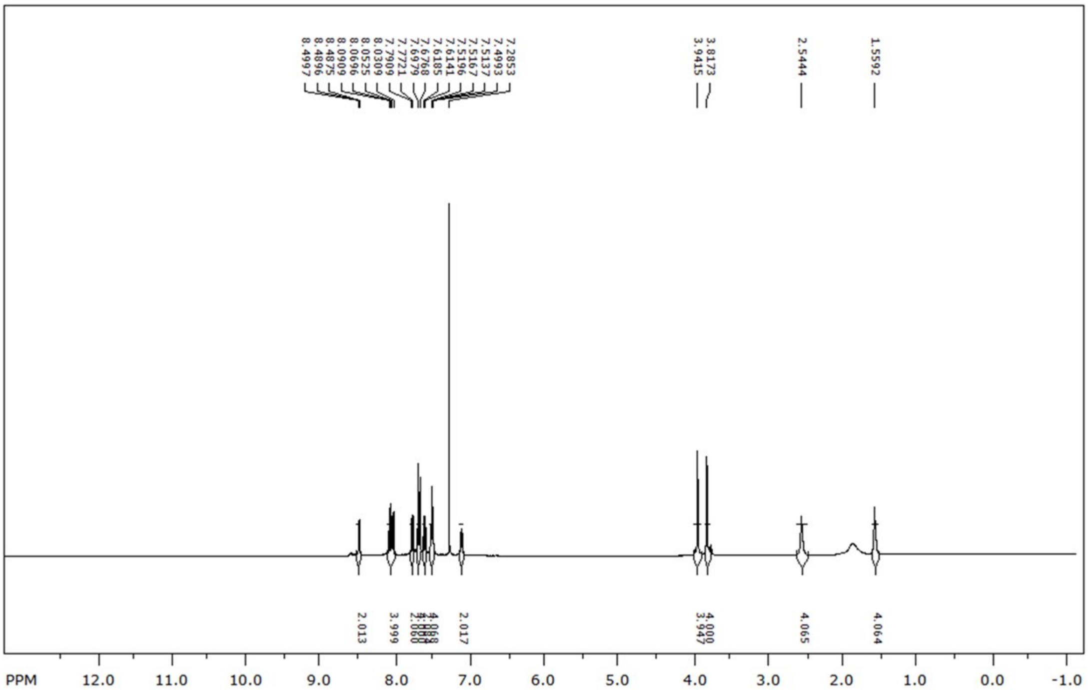

Fig. S4 ^{1}H NMR spectrum of **1** in $CDCl_3$.

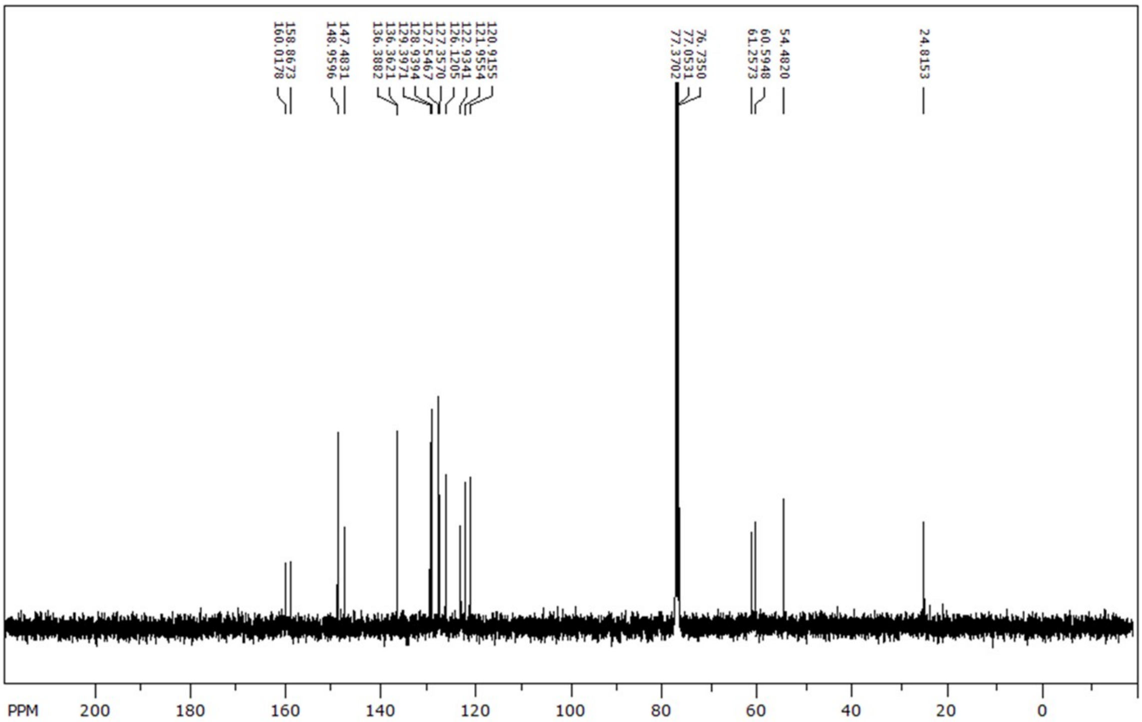

Fig. S5 ^{13}C NMR spectrum of **1** in $CDCl_3$.

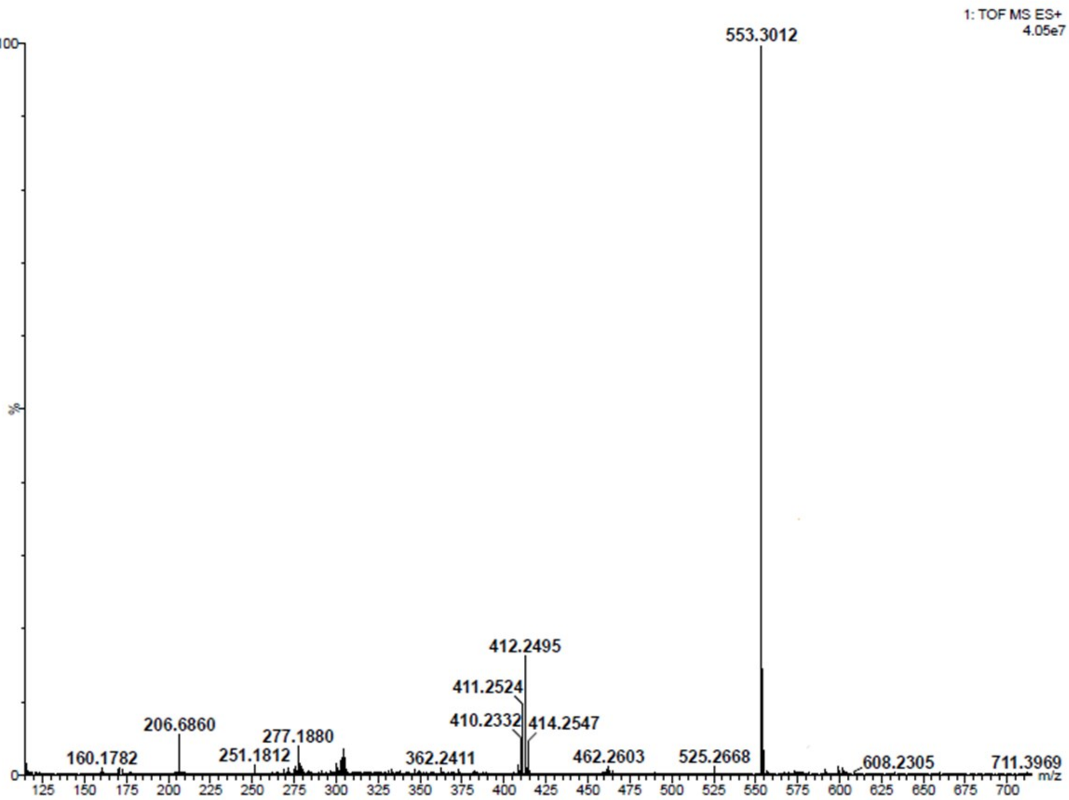

Fig. S6 HRMS spectrum of **1**.

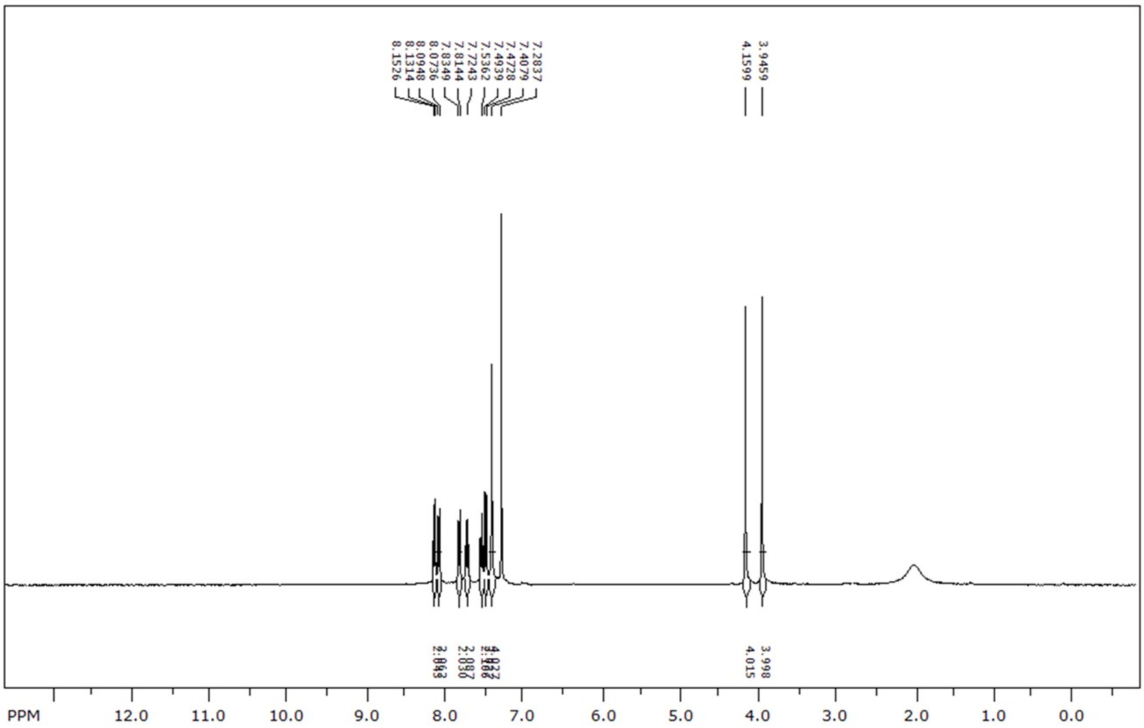

Fig. S7 ^{1}H NMR spectrum of **H_2bqxn** in $CDCl_3$.

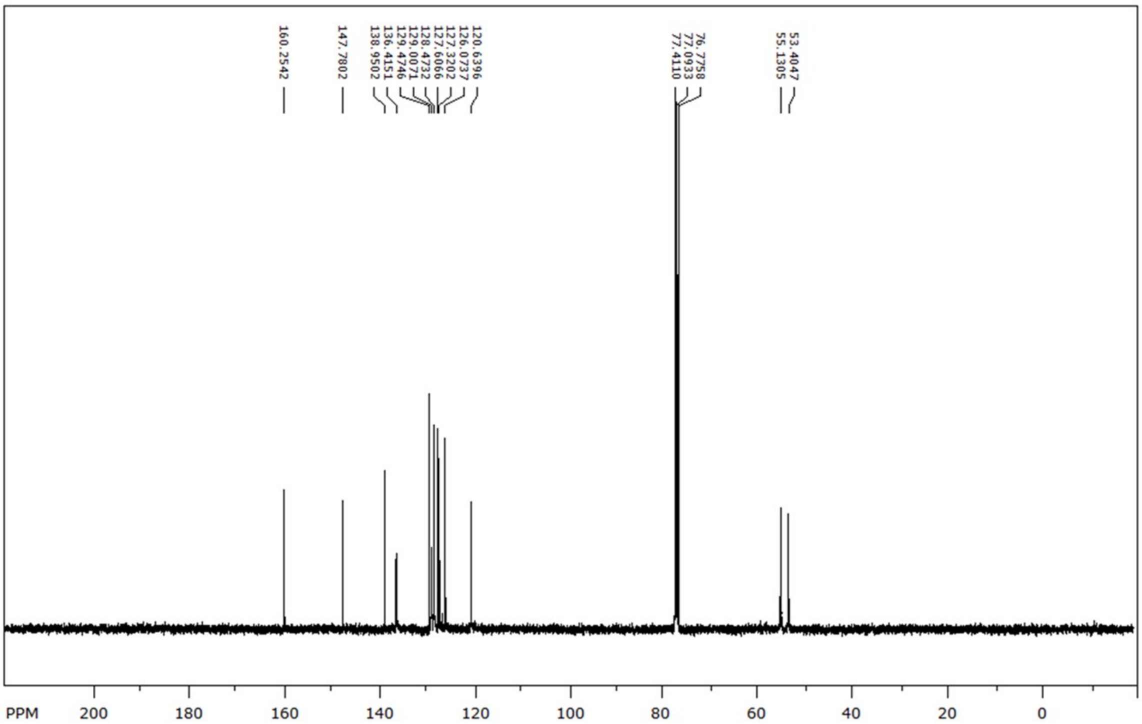

Fig. S8 ^{13}C NMR spectrum of **H_2bqxn** in $CDCl_3$.

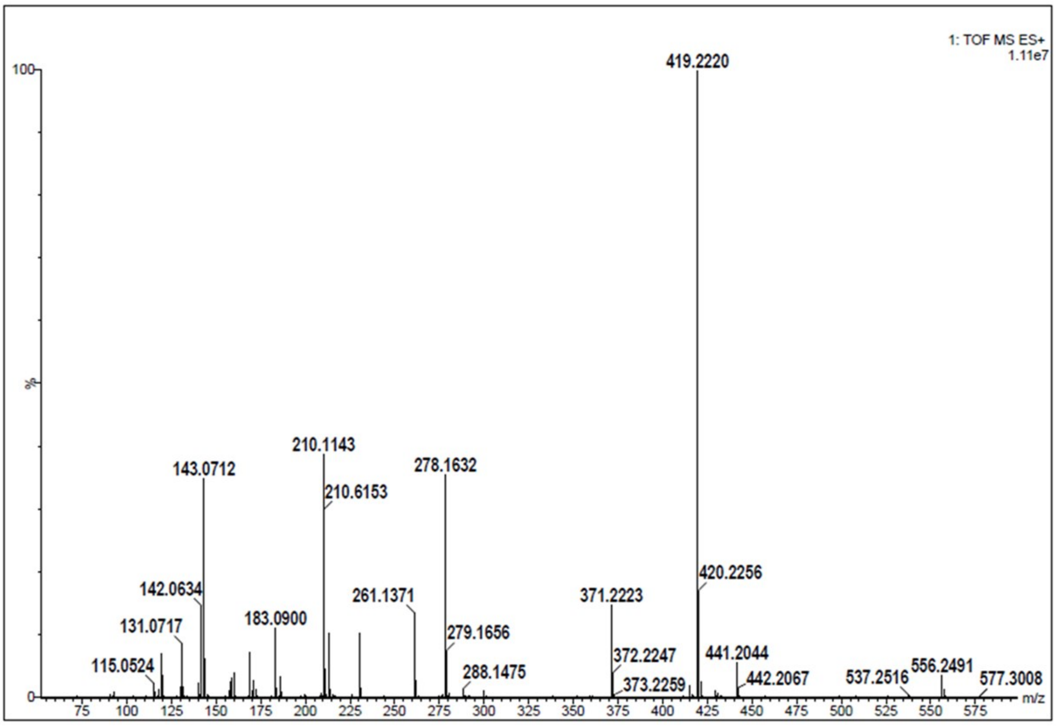

Fig. S9 HRMS spectrum of $\mathbf{H_2bqxn}$ in $CDCl_3$.

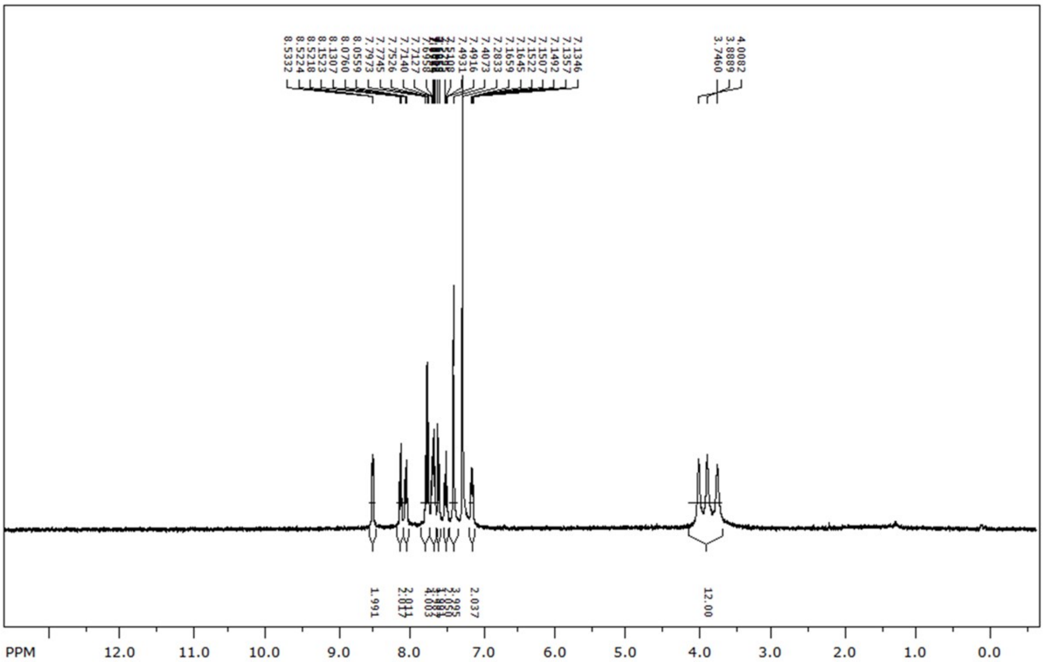

Fig. S10 ^{1}H NMR spectrum of **2** in $CDCl_3$.

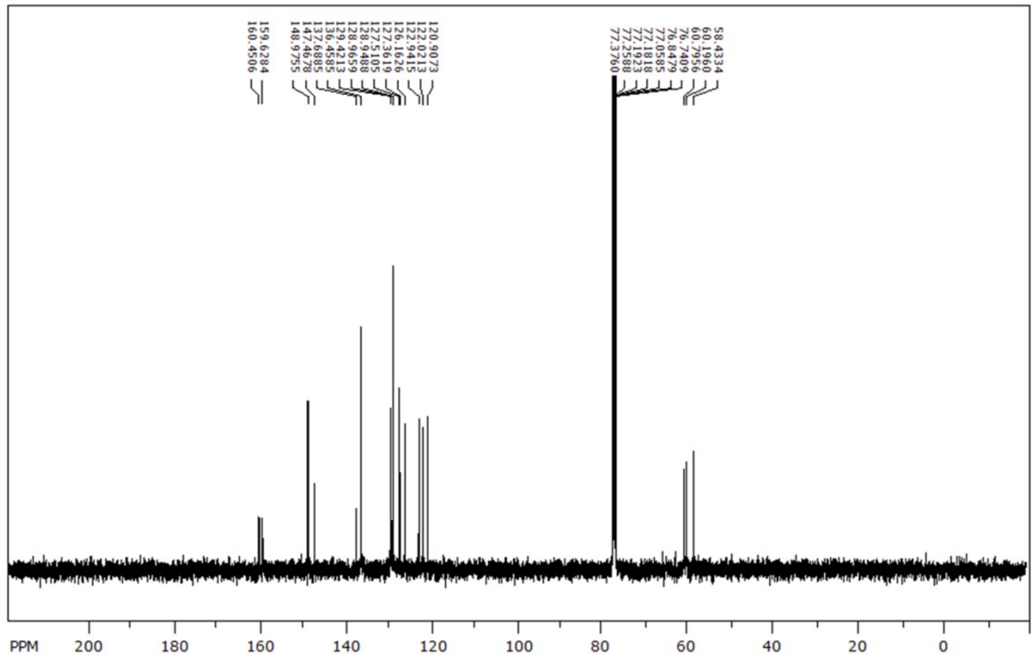

Fig. S11 ^{13}C NMR spectrum of **2** in $CDCl_3$.

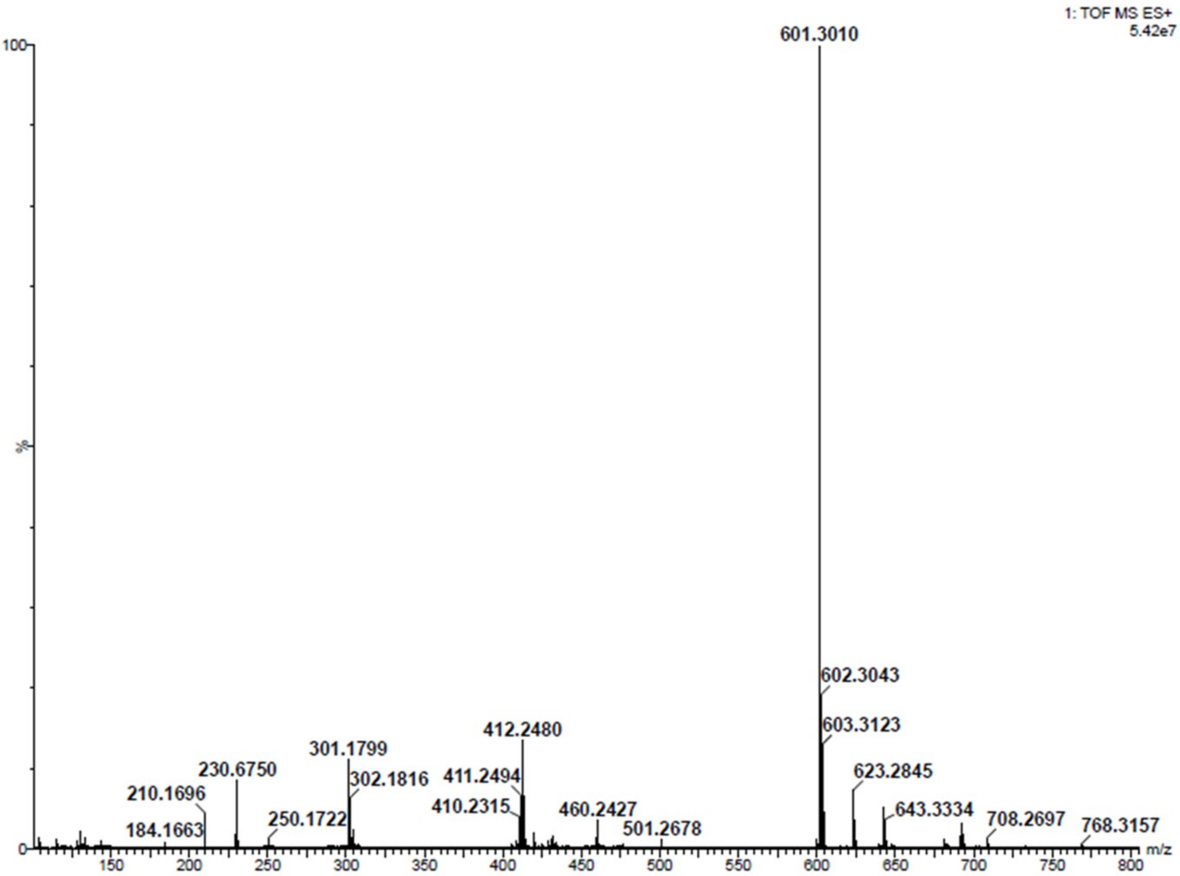

Fig. S12 HRMS spectrum of **2**.

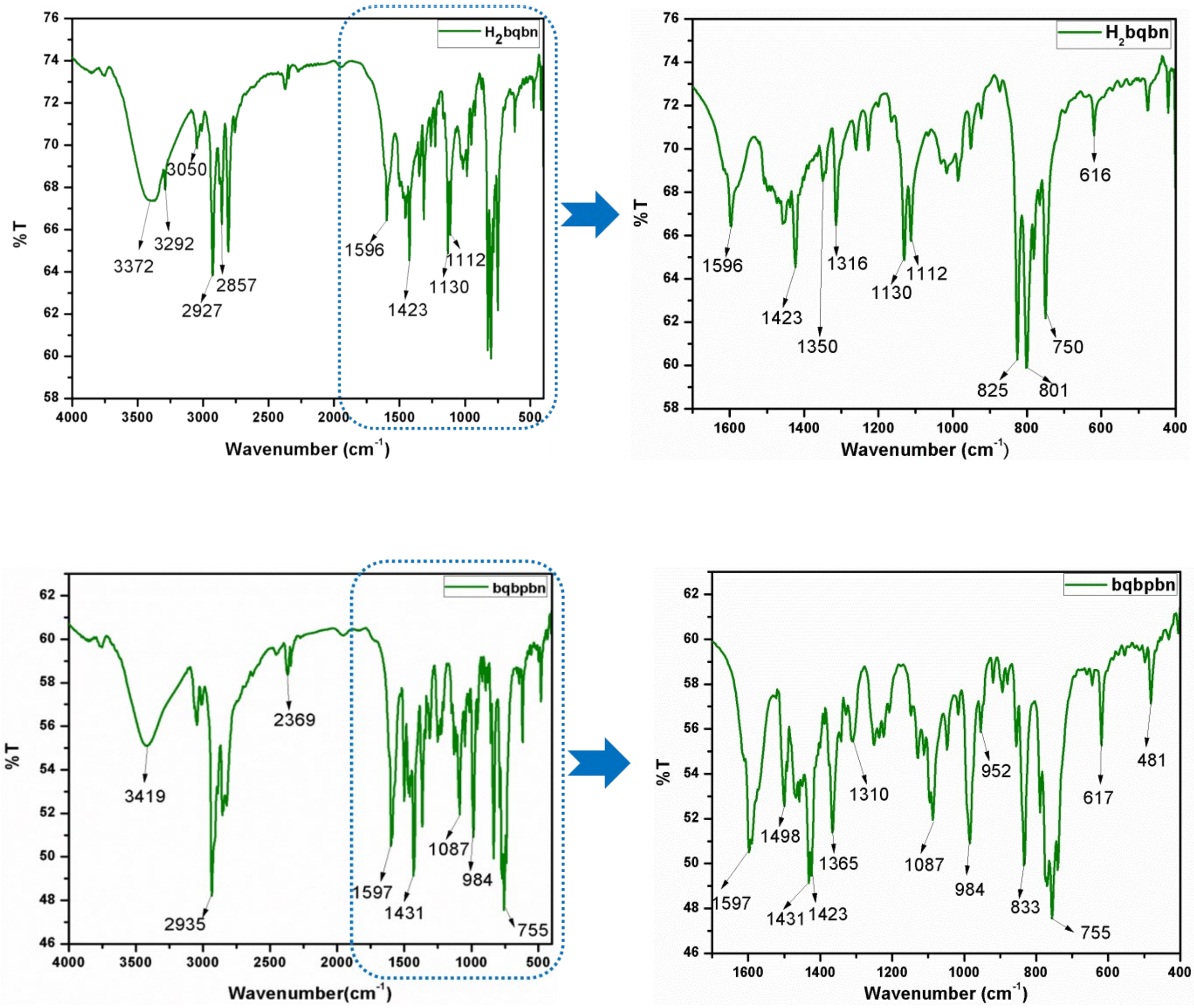

Fig. S13 FTIR spectra of **H_2bqbn** (top) and **1** (bottom).

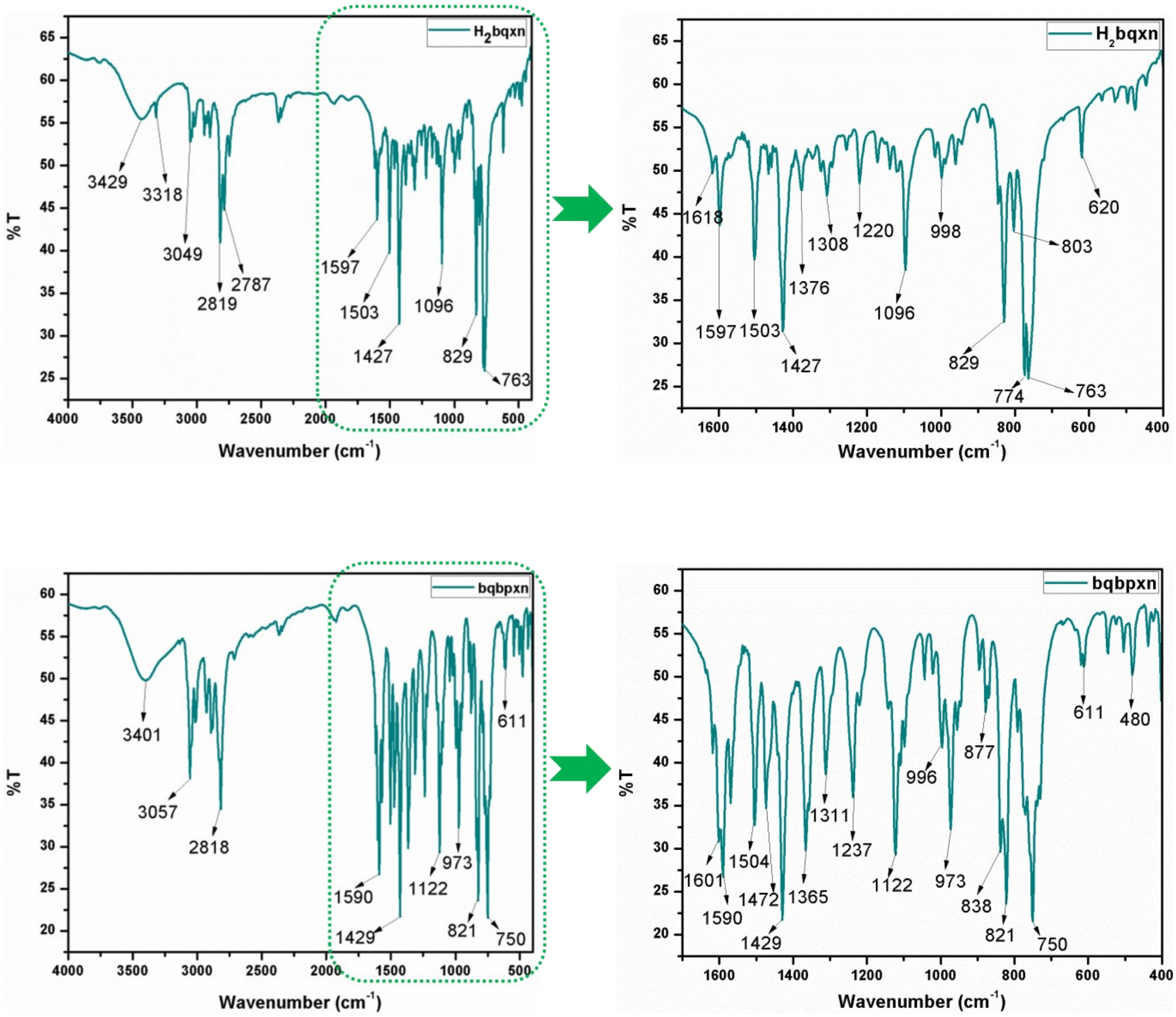

Fig. S14 FTIR spectra of **H_2bqxn** (top) and **2** (bottom).

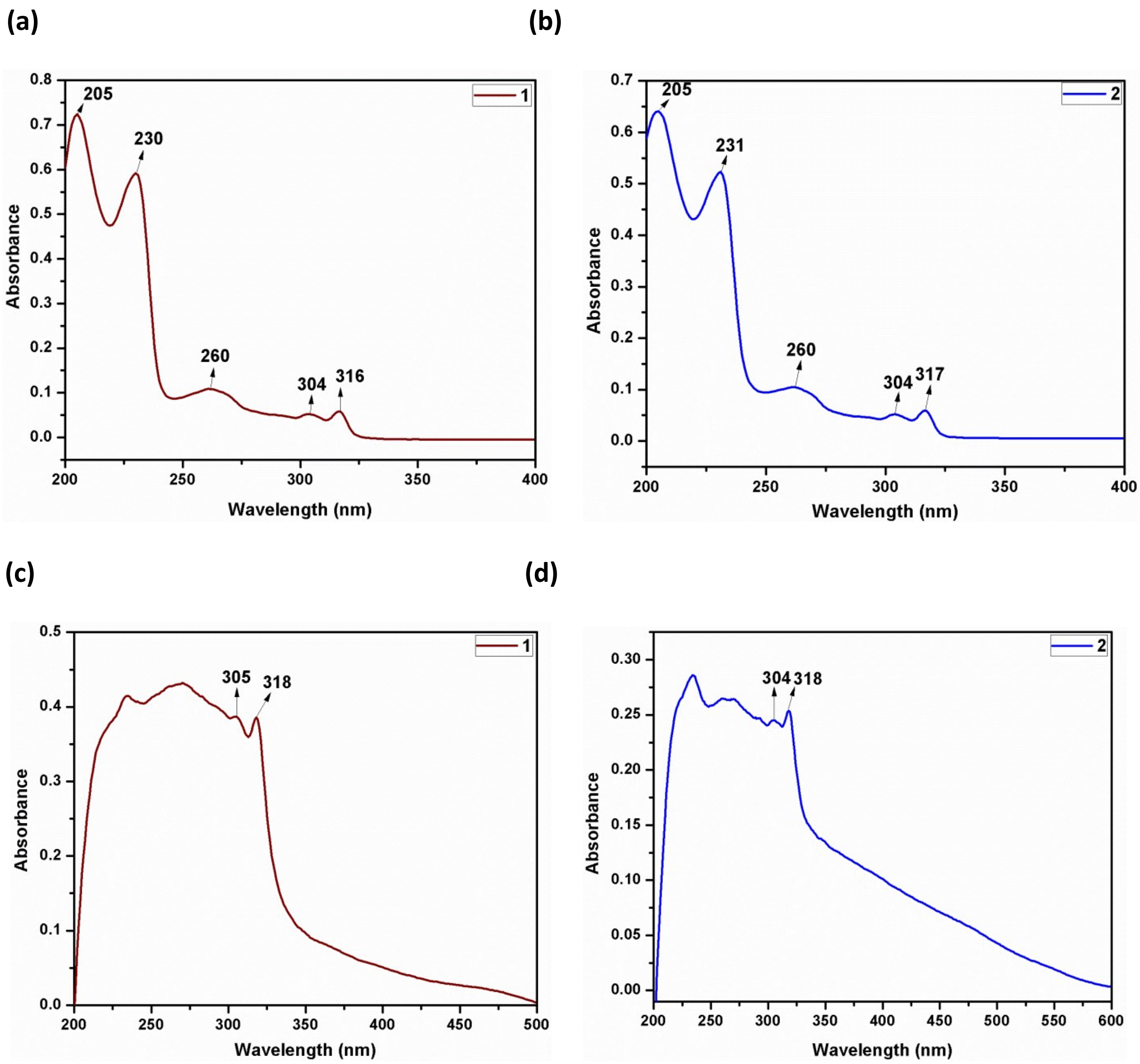

Fig. S15 UV-vis spectra of **1** (a) and **2** (b) in CH_3OH and solid-state diffuse-reflectance spectra of **1** (c) and **2** (d).

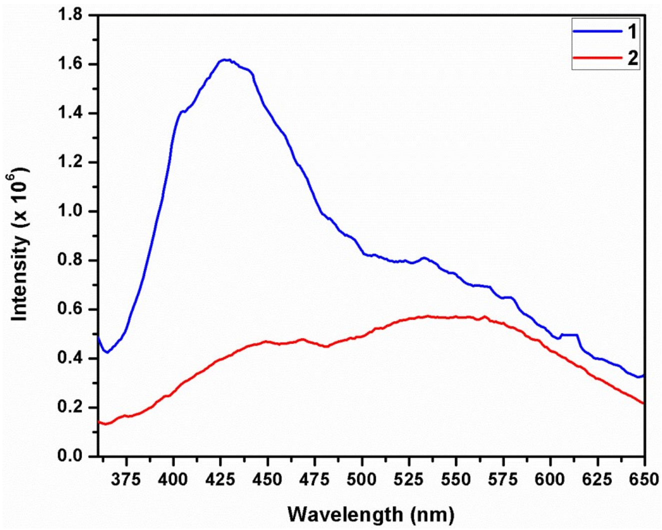

Fig. S16 Solid-state emission spectra of **1** and **2** (λ_{exc} = 340 nm).

Section-2: Fluorescence spectra of 1 and 2 in different solvents and in water with incremental addition of various NACs

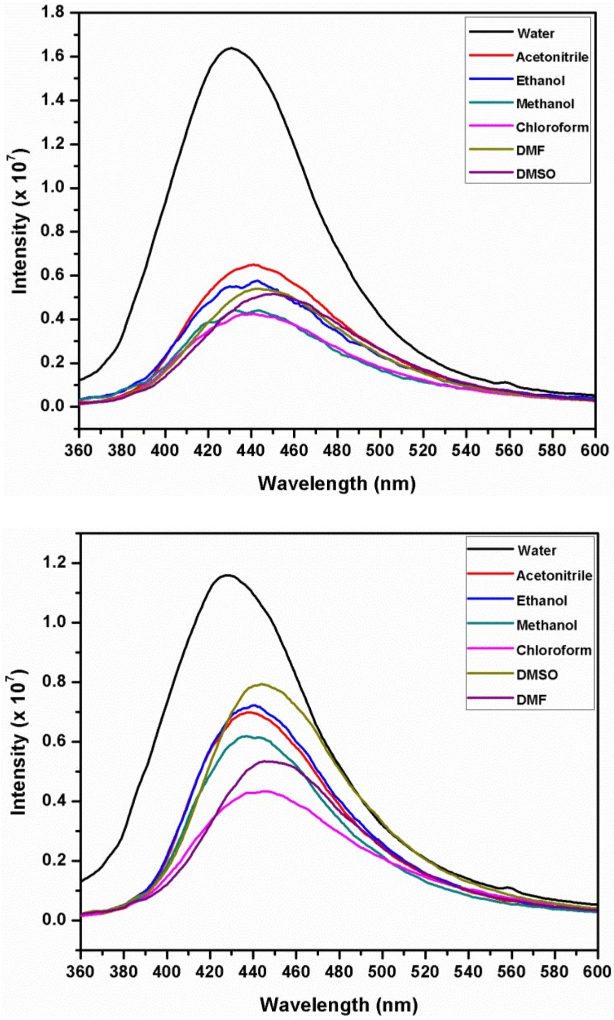

Fig. S17 Emission spectra of **1** (top) and **2** (bottom) (1 mg, 2 mL of different solvents (λ_{exc} = 340 nm).

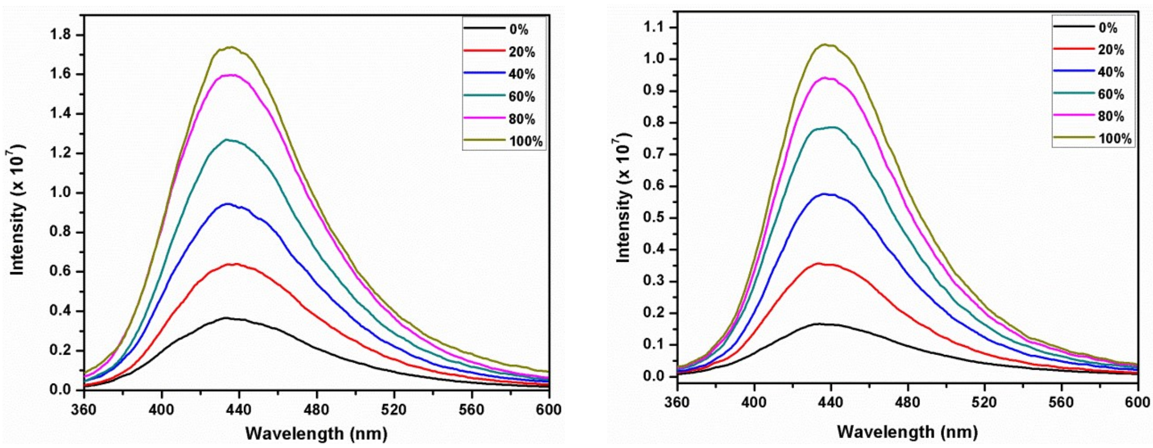

Fig. S18 Emission spectra of **1** (left) and **2** (right) (32 μM, THF) in presence of different volume fractions water (λ_{exc} = 340 nm).

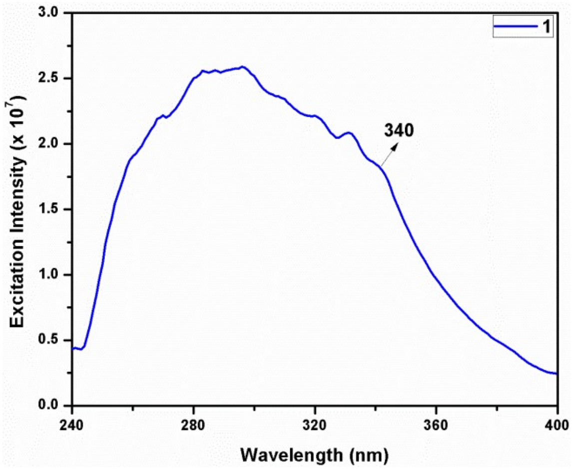

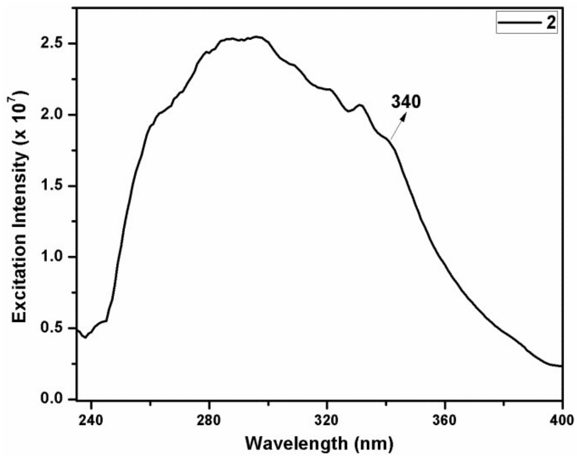

Fig. S19 Excitation spectra of **1** (top) and **2** (bottom) dispersed in 2 mL of milli-Q water.

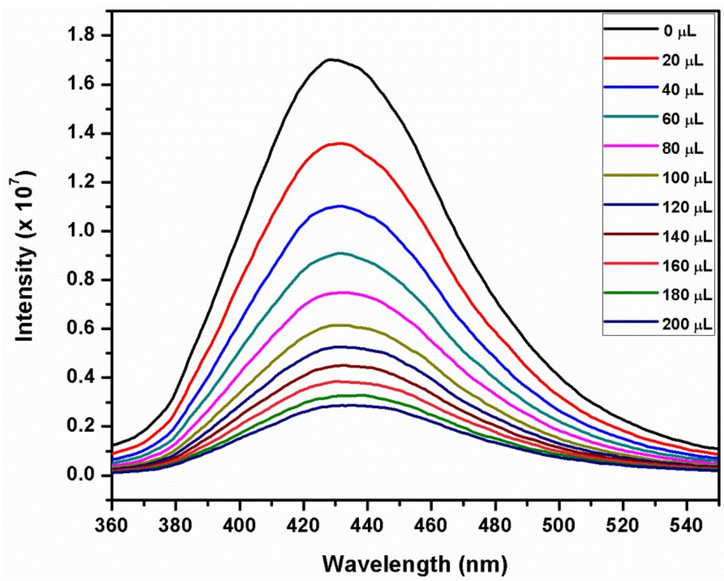

Fig. S20 Change in emission spectrum of **1** dispersed in water upon incremental addition of aqueous solution of 2,4-DNP (λ_{exc} = 340 nm).

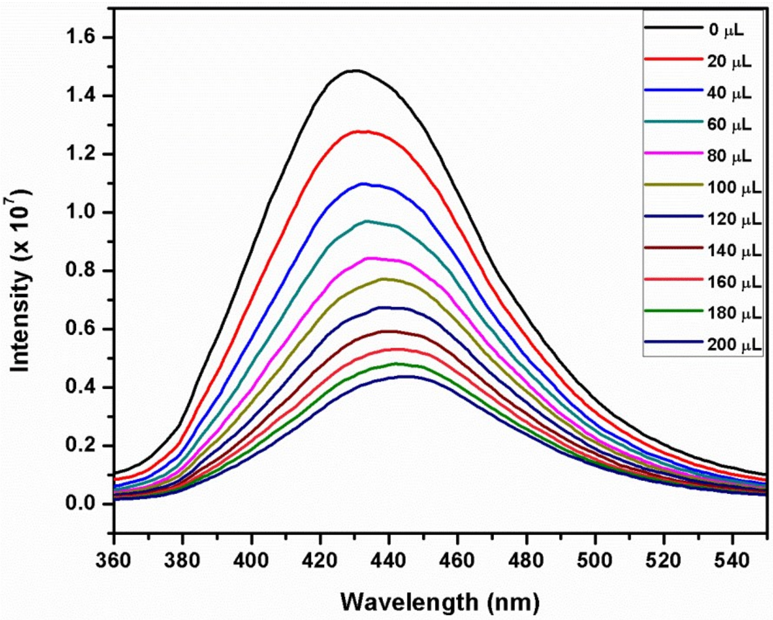

Fig. S21 Change in emission spectrum of **1** dispersed in water upon incremental addition of aqueous solution of 4-NP (λ_{exc} = 340 nm).

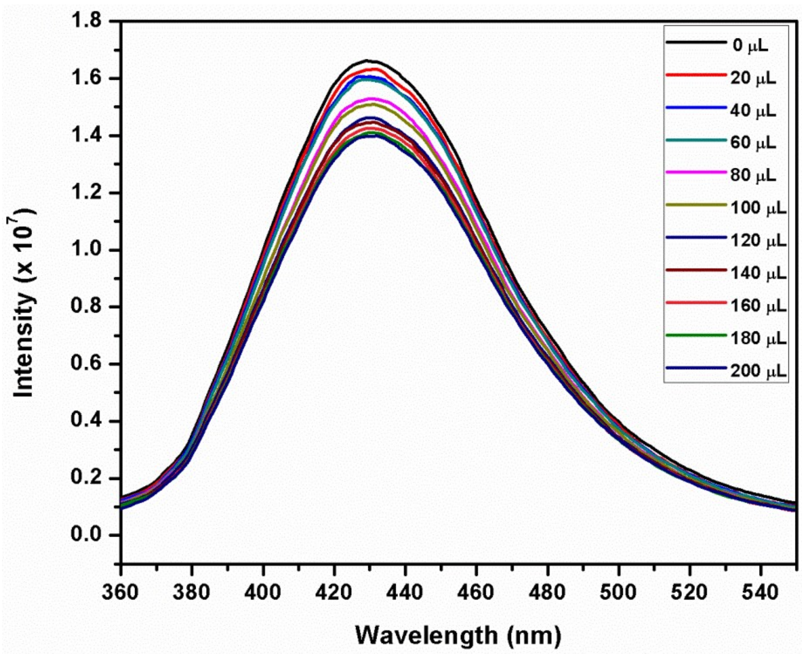

Fig. S22 Change in emission spectrum of **1** dispersed in water upon incremental addition of aqueous solution of TNT (λ_{exc} = 340 nm).

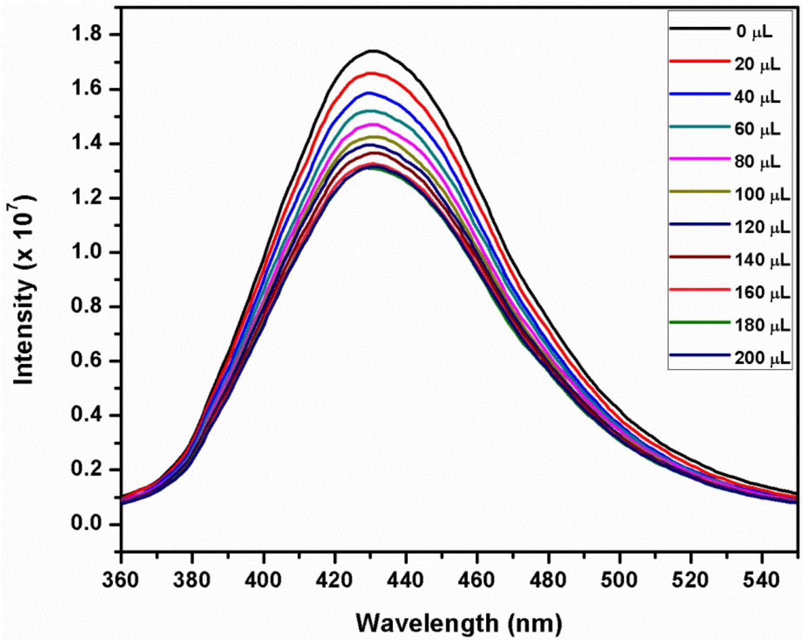

Fig. S23 Change in emission spectrum of **1** dispersed in water upon incremental addition of aqueous solution of 2,6-DNT (λ_{exc} = 340 nm).

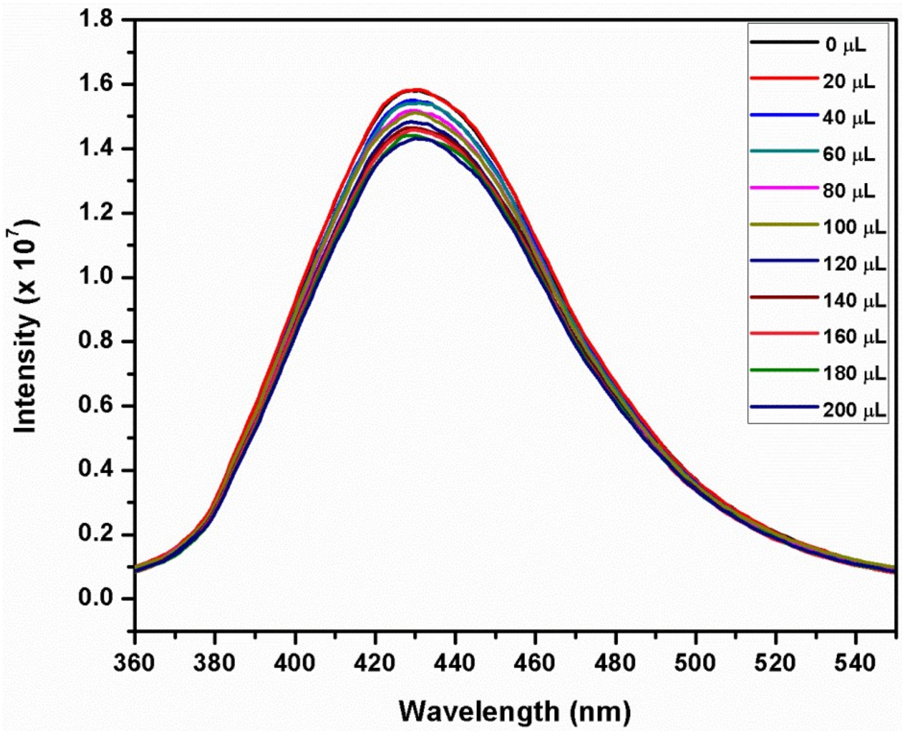

Fig. S24 Change in emission spectrum of **1** dispersed in water upon incremental addition of aqueous solution of 2,4-DNT (λ_{exc} = 340 nm).

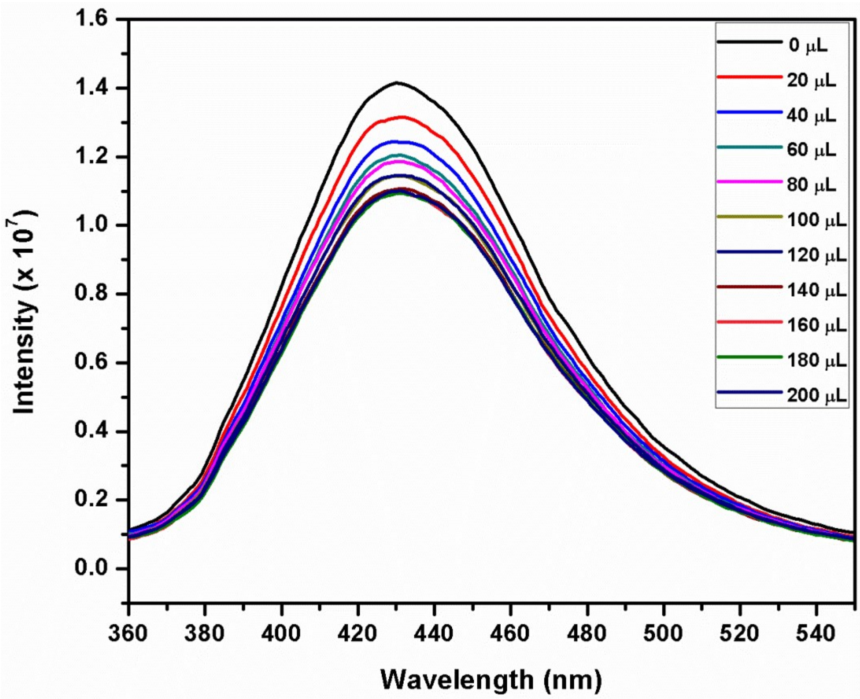

Fig. S25 Change in emission spectrum of **1** dispersed in water upon incremental addition of aqueous solution of 1,3-DNB (λ_{exc} = 340 nm).

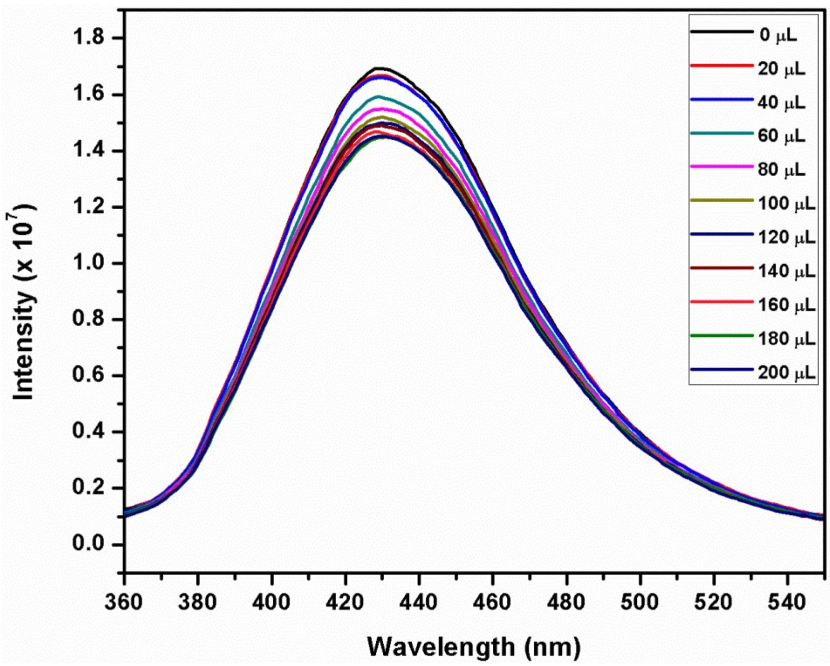

Fig. S26 Change in emission spectrum of **1** dispersed in water upon incremental addition of aqueous solution of NB (λ_{exc} = 340 nm).

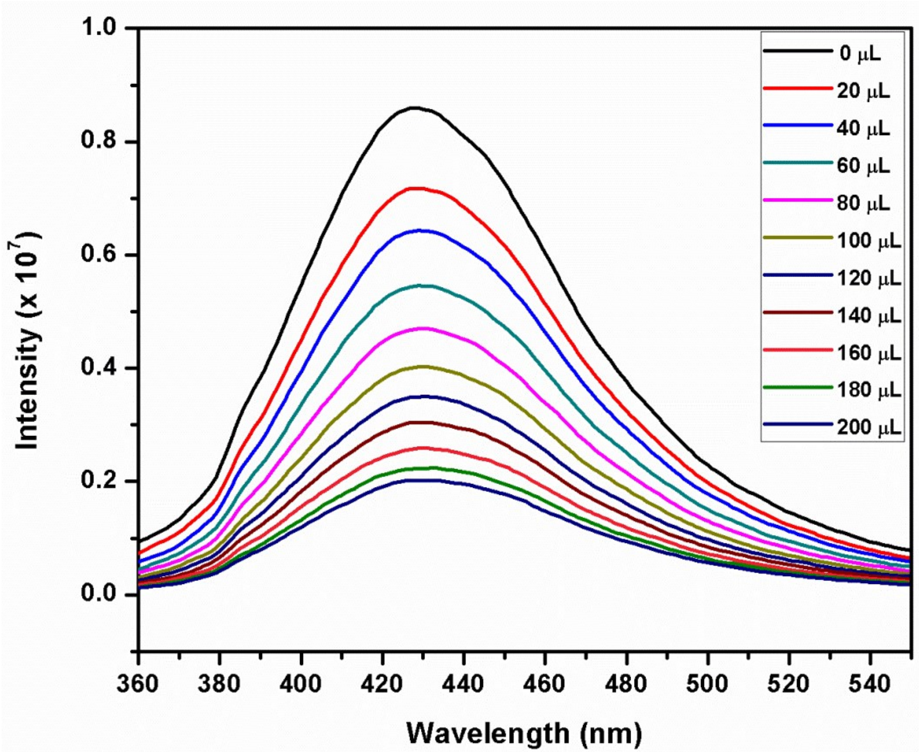

Fig. S27 Change in emission spectrum of **2** dispersed in water upon incremental addition of aqueous solution of 2,4-DNP (λ_{exc} = 340 nm).

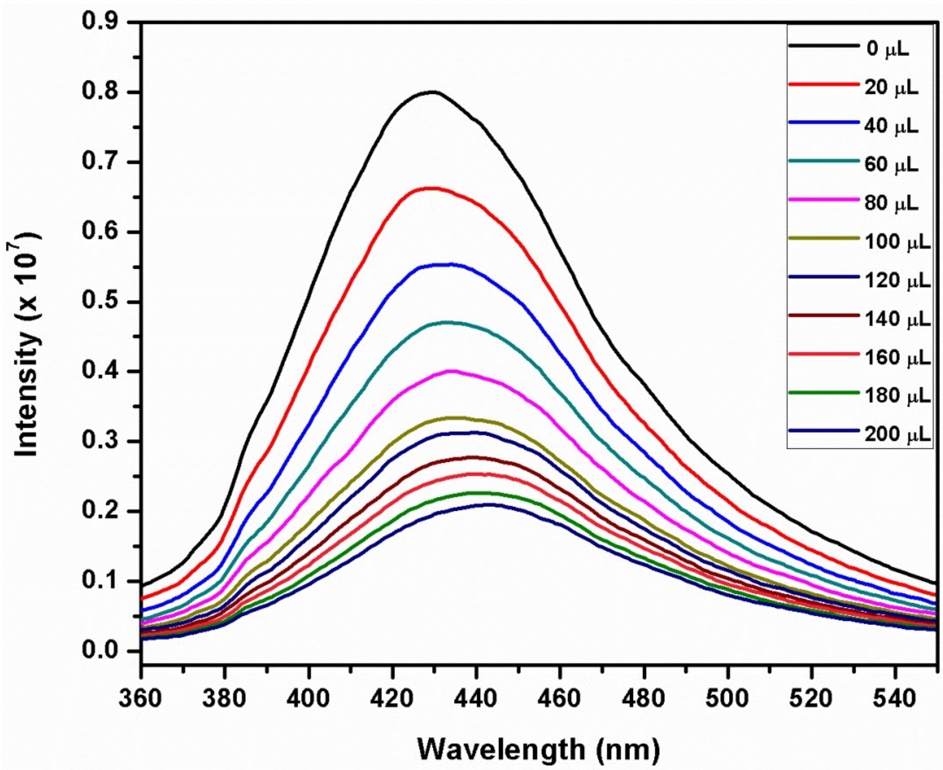

Fig. S28 Change in emission spectrum of **2** dispersed in water upon incremental addition of aqueous solution of 4-NP (λ_{exc} = 340 nm).

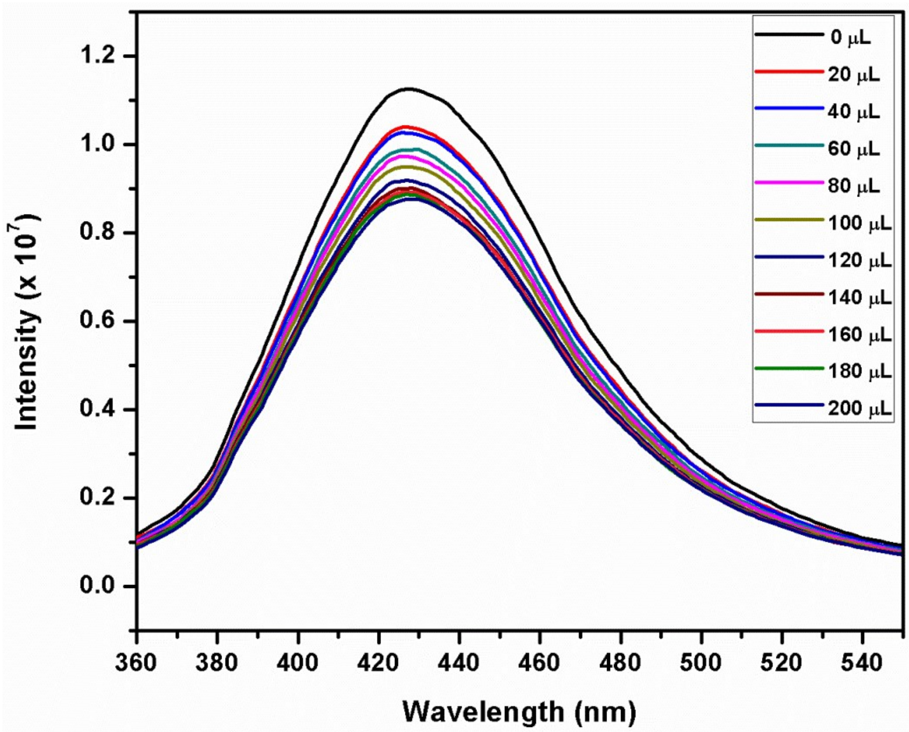

Fig. S29 Change in emission spectrum of **2** dispersed in water upon incremental addition of aqueous solution of TNT (λ_{exc} = 340 nm).

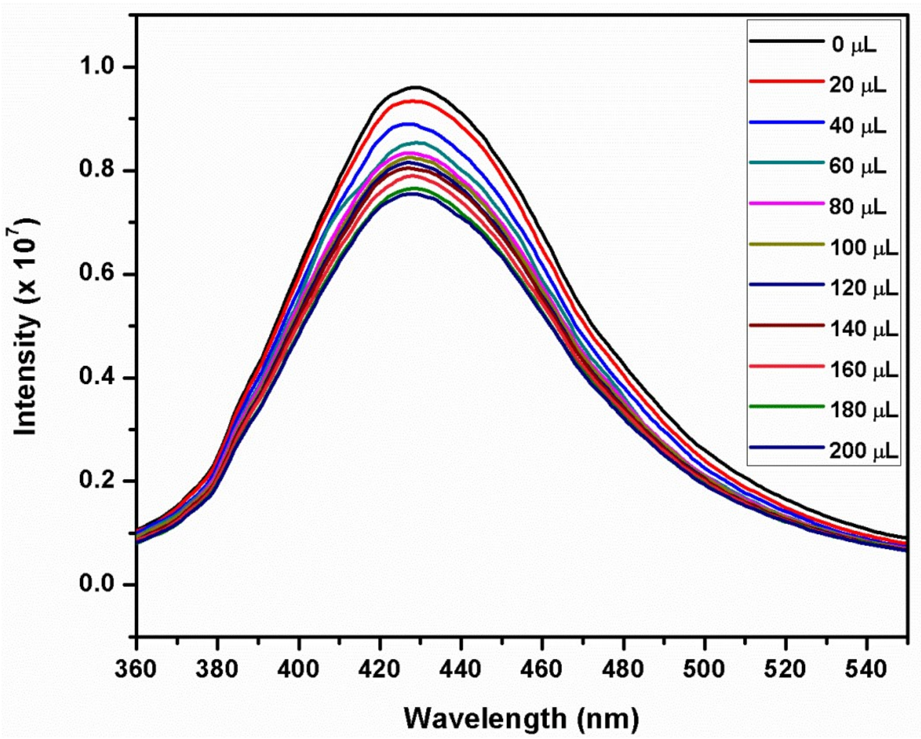

Fig. S30 Change in emission spectrum of **2** dispersed in water upon incremental addition of aqueous solution of 2,6-DNT (λ_{exc} = 340 nm).

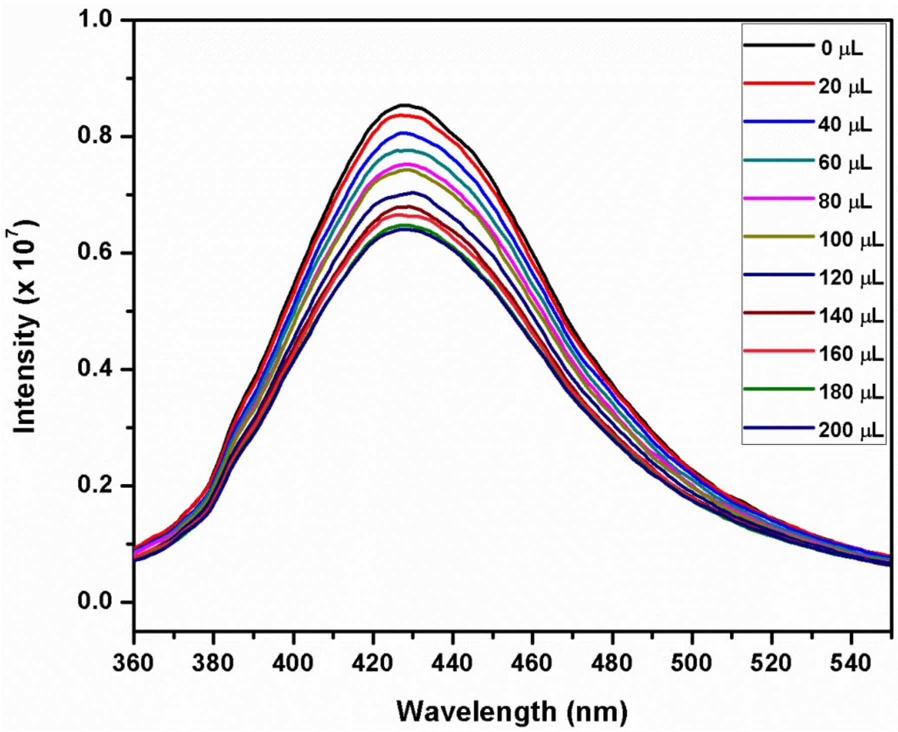

Fig. S31 Change in emission spectrum of **2** dispersed in water upon incremental addition of aqueous solution of 2,4-DNT (λ_{exc} = 340 nm).

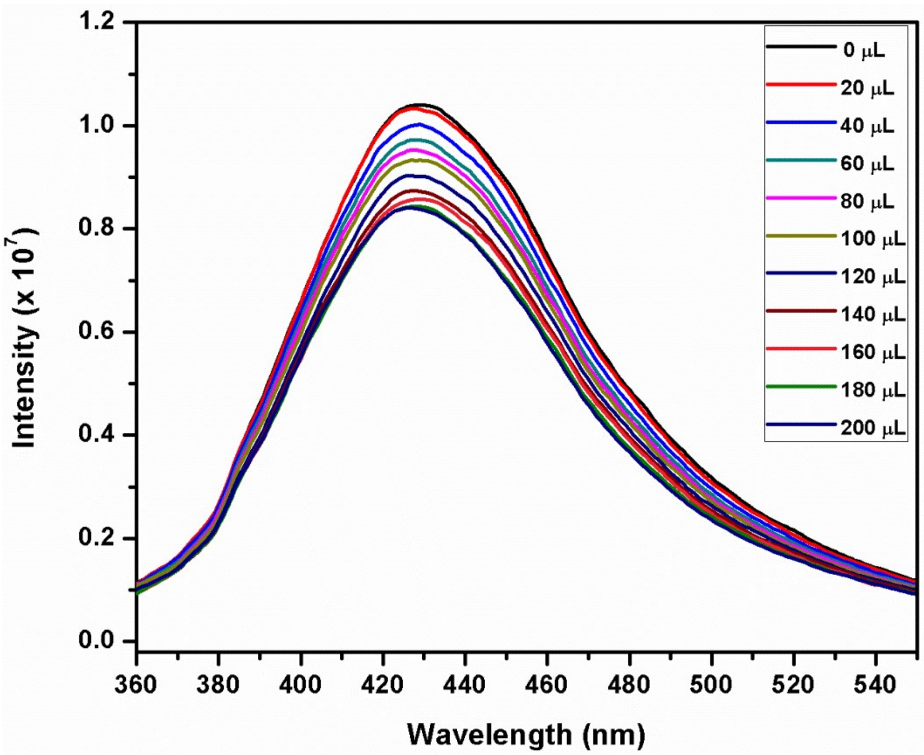

Fig. S32 Change in emission spectrum of **2** dispersed in water upon incremental addition of aqueous solution of 1,3-DNB (λ_{exc} = 340 nm).

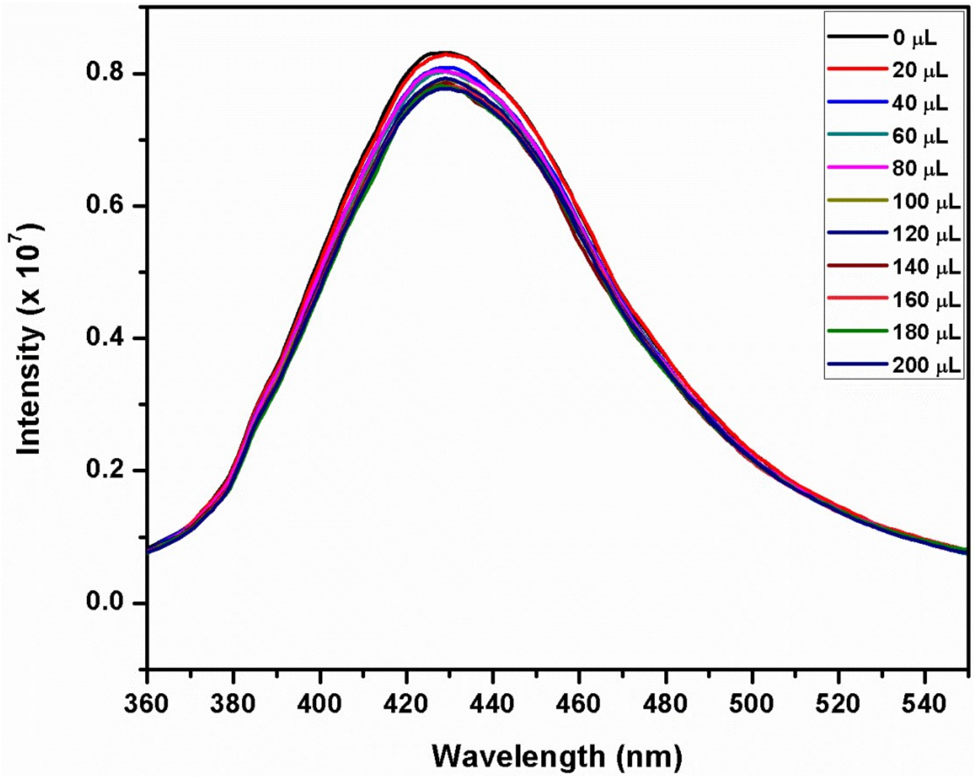

Fig. S33 Change in emission spectrum of **2** dispersed in water upon incremental addition of aqueous solution of NB (λ_{exc} = 340 nm).

Section-3: Stern-Volmer plots for NACs in 1 and 2

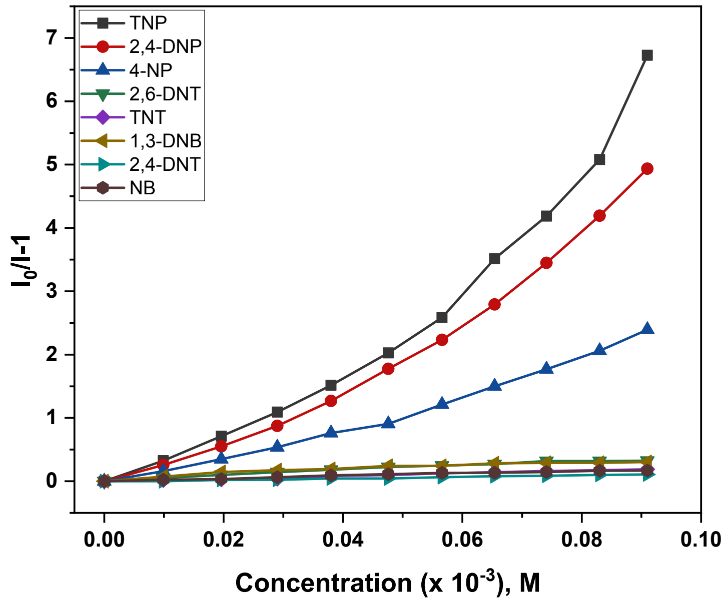

Fig. S34 Stern-Volmer plots of different NACs in **1**.

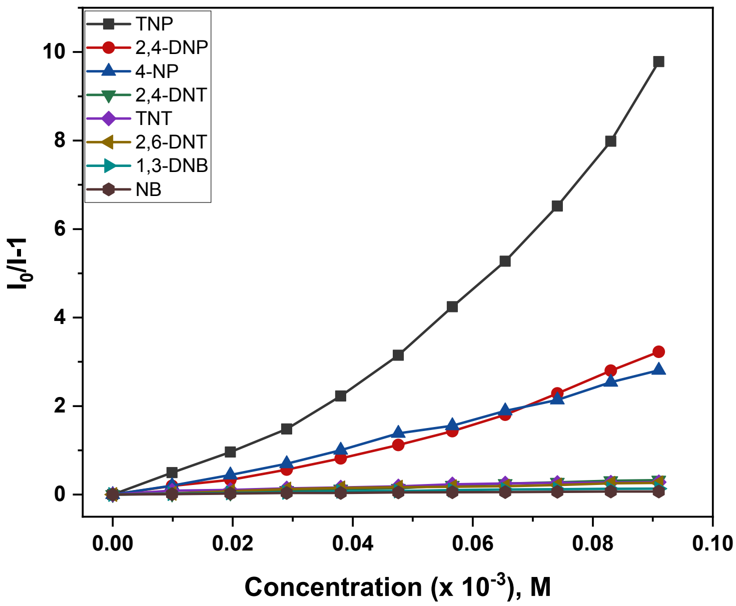

Fig. S35 Stern-Volmer plots of different NACs in **2**.

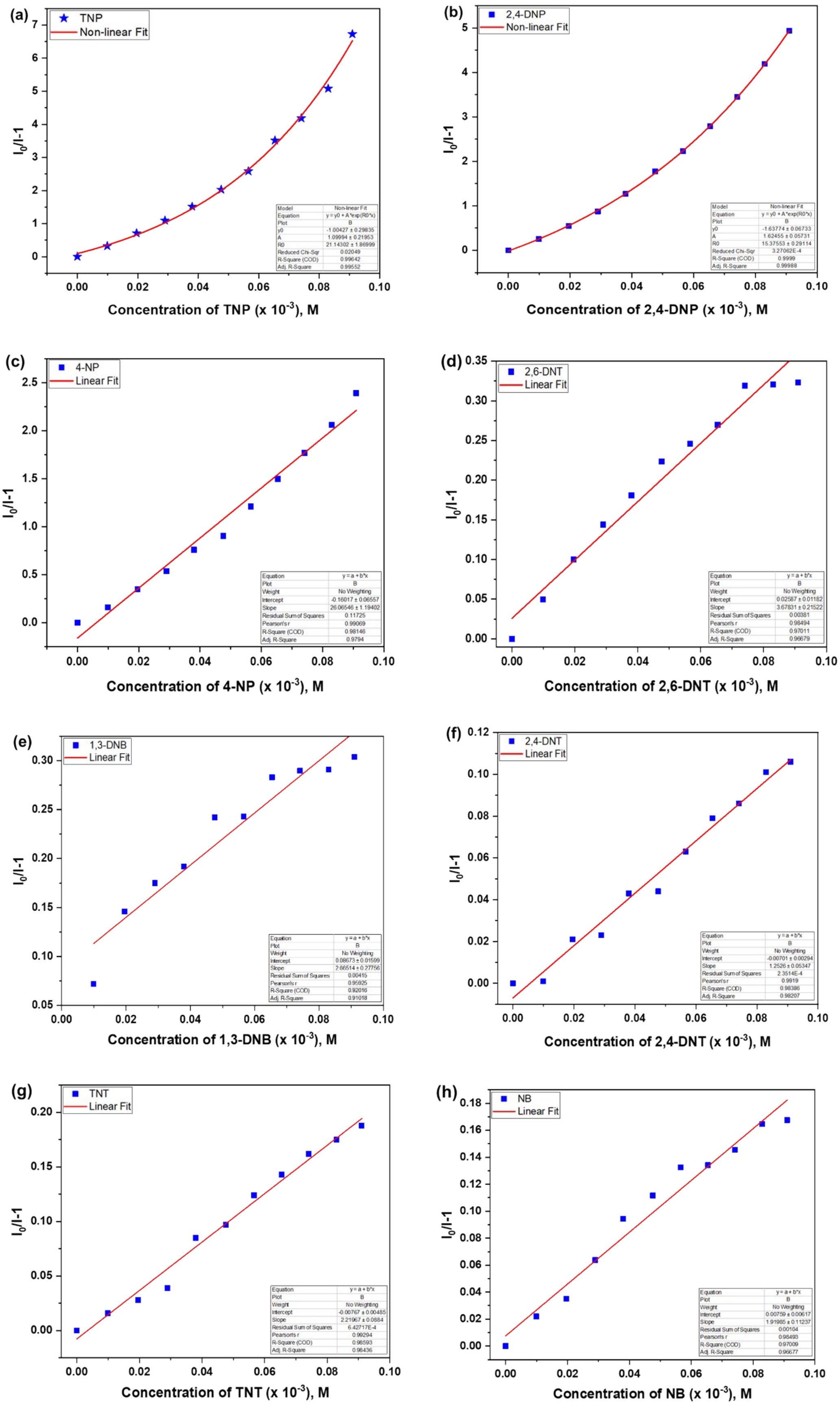

Fig. S36 Fitted Stern-Volmer plots of (a) TNP, (b) 2,4-DNP, (c) 4-NP, (d) 2,6-DNT, (e) 1,3-DNB, (f) 2,4-DNT, (g) TNT and (h) NB in **1**.

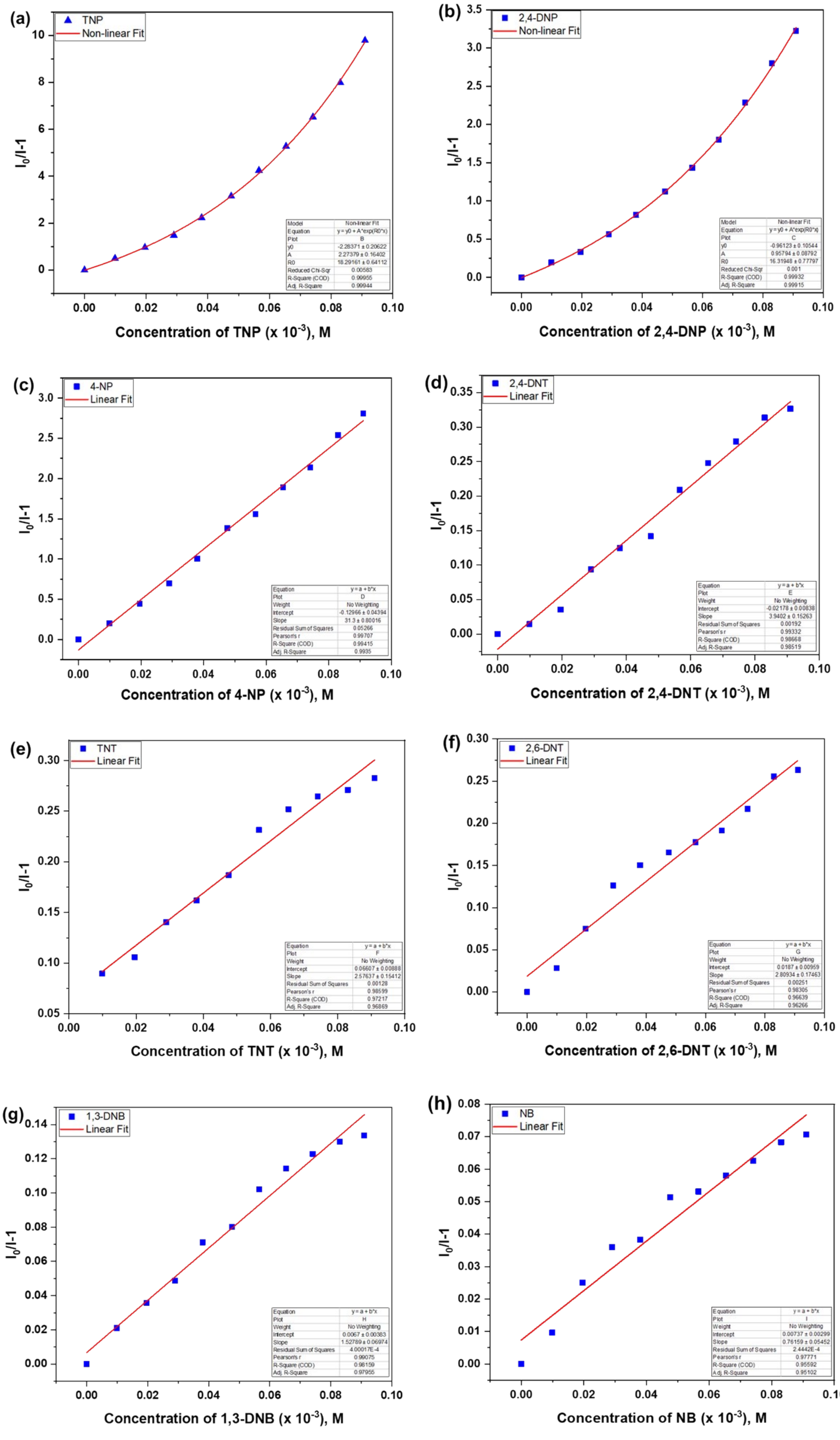

Fig. S37 Fitted Stern-Volmer plots of (a) TNP, (b) 2,4-DNP, (c) 4-NP, (d) 2,4-DNT, (e) TNT, (f) 2,6-DNT, (g) 1,3-DNB and (h) NB in **2**.

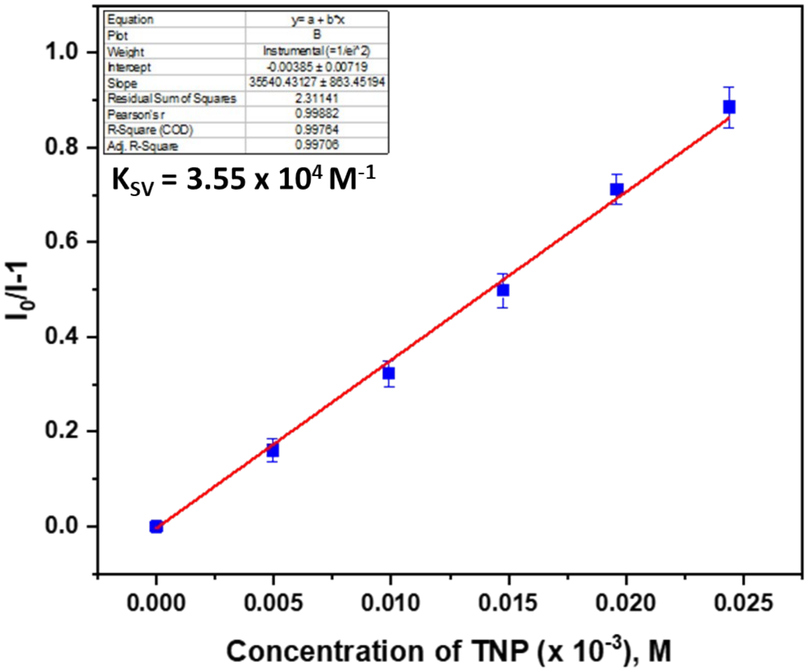

Fig. S38 Stern-Volmer (SV) plot for TNP in **1**. The relative fluorescence intensity is linear with TNP concentration in the range of 0 – 0.025 mM, $I_0/I = 1 + 35540.43[TNP]$ ($R^2 = 0.997$).

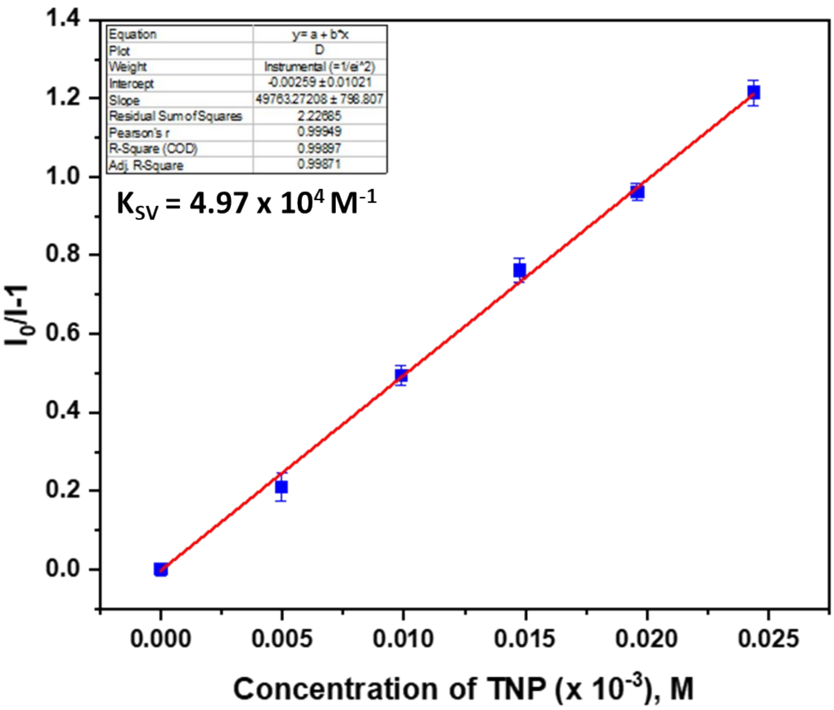

Fig. S39 Stern-Volmer (SV) plot for TNP in **2**. The relative fluorescence intensity is linear with TNP concentration in the range of 0 – 0.025 mM, $I_0/I = 1 + 49763.27[TNP]$ ($R^2 = 0.999$).

Section-4: Detection limit calculation for TNP in 1 and 2

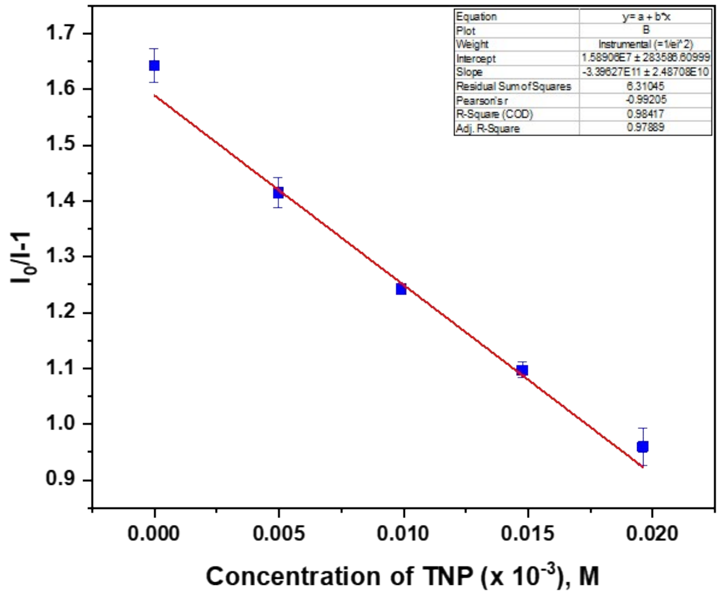

Fig. S40 Determination of detection limit through fitting of the linear region of fluorescence intensity of **1** upon incremental addition of TNP to it at λ_{emi} = 429 nm (upon λ_{exc} = 340 nm) (R^2 = 0.984).

Table S1: Calculation of Standard Deviation of 1.

Blank Readings (**1**)	Emission Intensity
Reading 1	1.662E7
Reading 2	1.746E7
Reading 3	1.643E7
Reading 4	1.588E7
Reading 5	1.701E7
Reading 6	1.643E7
Reading 7	1.603E7
Reading 8	1.745E7
Reading 9	1.735E7
Reading 10	1.727E7
Standard Deviation (σ)	592806

Determination of Detection Limit of TNP in 1:

Detection limit was calculated using the following equation:
Detection limit = $3\sigma/m$
Where 'σ' is the calculated standard deviation from ten blank measurements and 'm' is the slope obtained from the plot of fluorescence emission with increasing concentration of TNP.

Slope from Graph (m)	$3.3962 \times 10^{11}\ M^{-1}$
Detection Limit ($3\sigma/m$)	5.236 μM (**1.2 ppm**)

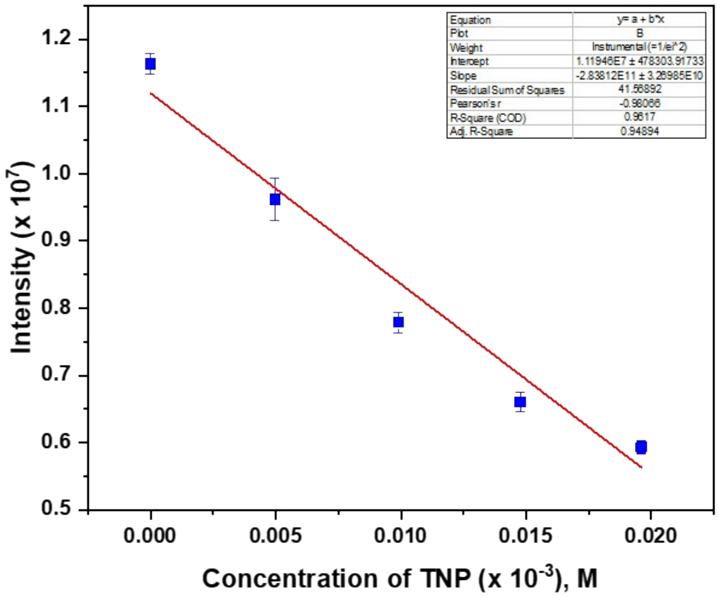

Fig. S41 Determination of detection limit through fitting of the linear region of fluorescence intensity of **2** upon incremental addition of TNP to it at λ_{emi} = 427 nm (upon λ_{exc} = 340 nm) (R^2 = 0.961).

Table S2: Calculation of Standard Deviation of 2.

Blank Readings (**2**)	Emission Intensity
Reading 1	1.130E7
Reading 2	1.101E7
Reading 3	1.121E7
Reading 4	1.133E7
Reading 5	1.111E7
Reading 6	1.137E7
Reading 7	1.110E7
Reading 8	1.132E7
Reading 9	1.117E7
Reading 10	1.101E7
Standard Deviation (σ)	134281.87

Determination of Detection Limit of TNP in 2:

Detection limit was calculated using the following equation:
Detection limit = 3σ/m
Where 'σ' is the calculated standard deviation from ten blank measurements and 'm' is the slope obtained from the plot of fluorescence emission with increasing concentration of TNP.

Slope from Graph (m)	$2.8381 \times 10^{11}\ M^{-1}$
Detection Limit (3σ/m)	1.41 μM (**0.3 ppm**)

Section-5: Energy minimized structures and HOMO-LUMO energy level diagrams of 1, 2 and NACs

(a)

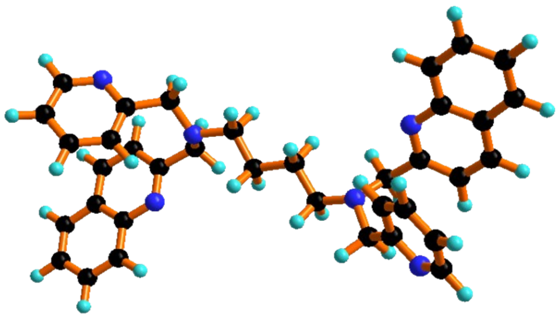

(b)

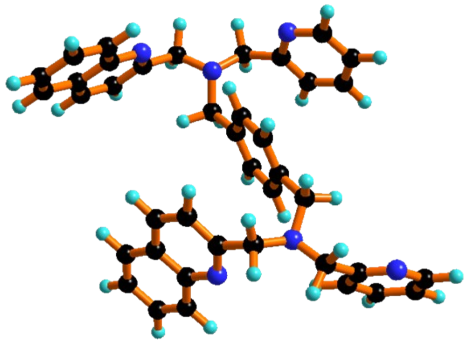

Fig. S42 Energy minimized structures of **1** (a) and **2** (b). (Color code: carbon in black, nitrogen in blue and hydrogen in sky blue).

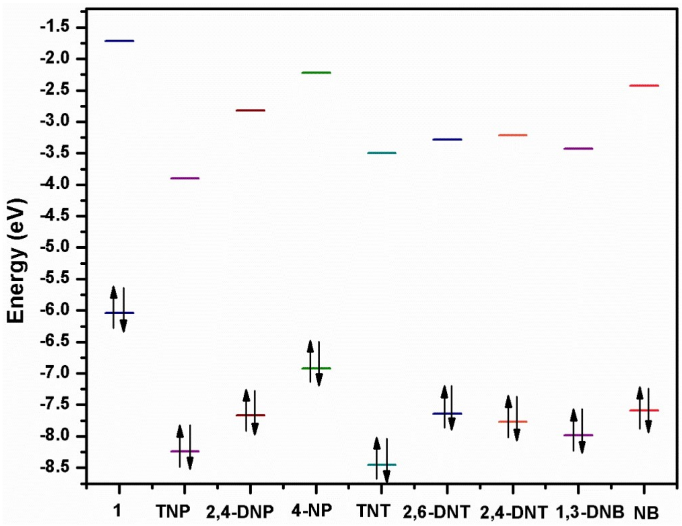

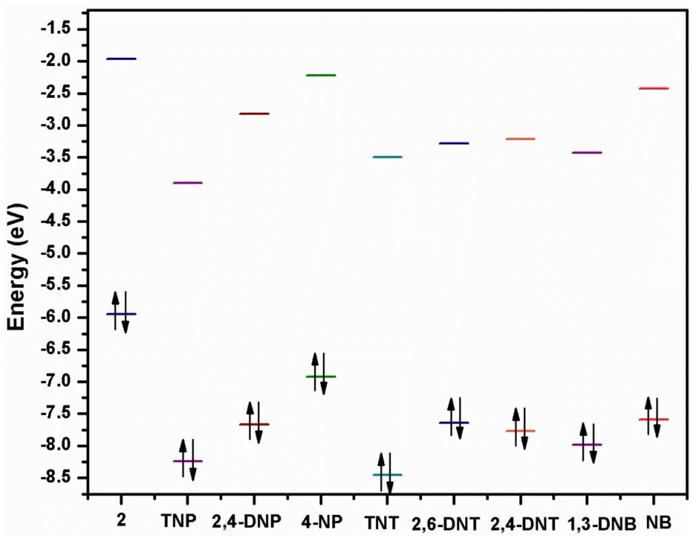

Fig. S43 HOMO and LUMO energy level diagrams of **1** (top), **2** (bottom) and the electron-deficient NACs.

Section-6: Hydrolytic and chemical stability confirmed by PXRD and FE-SEM

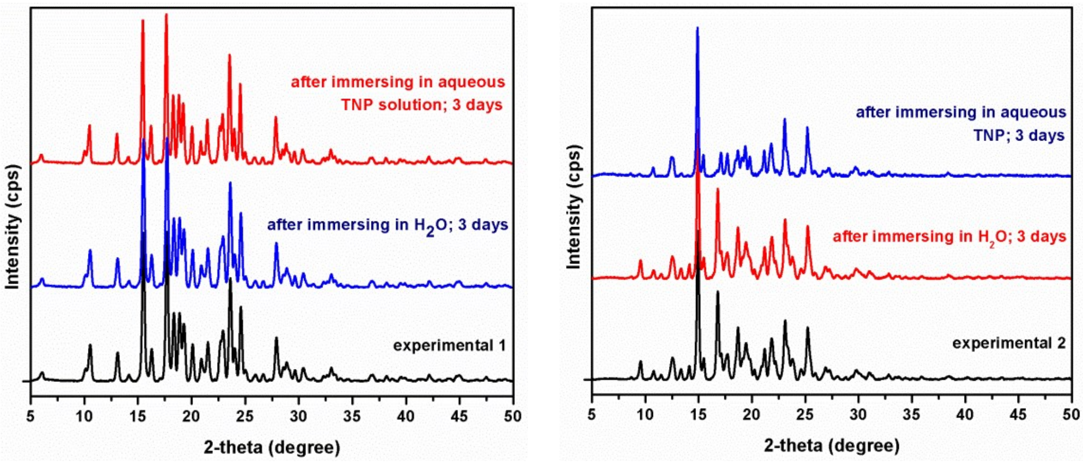

Fig. S44 PXRD profiles of **1** (left) and **2** (right) before and after immersing in water and aqueous TNP solution.

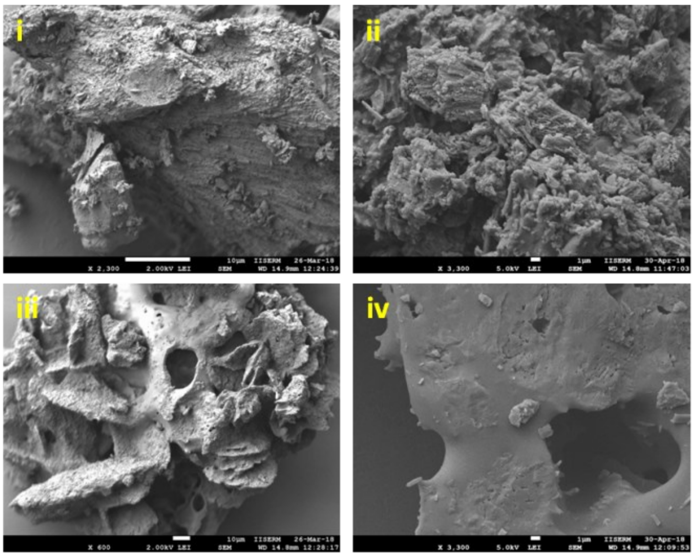

Fig. 45 FE-SEM images of **1** (i, ii) and **2** (iii, iv) before and after immersing in aqueous solution of TNP (1 mM), respectively.

Section-7: Recyclability test

(a)

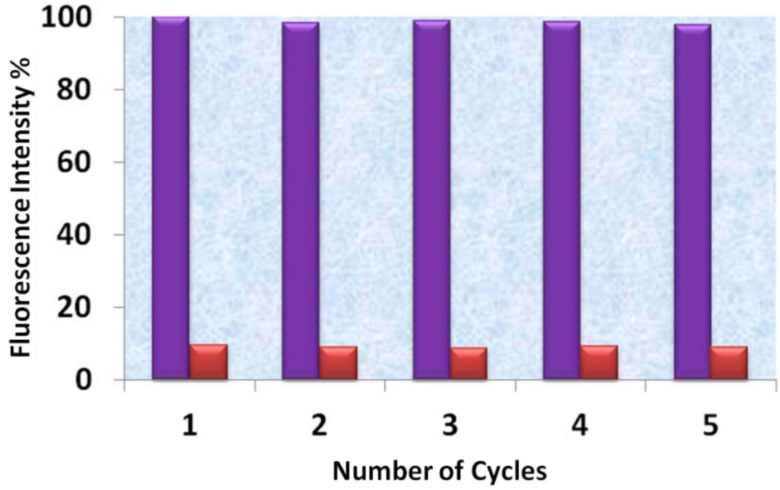

(b)

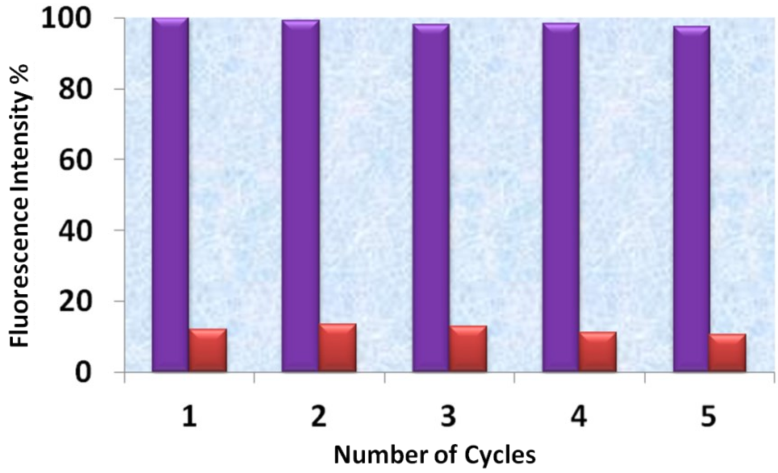

Fig. S46 Bar diagrams depicting the recyclability of (a) **1** and (b) **2** over five cycles after quenching experiment with TNP (dark red bars = initial intensity, blue bars = intensity after addition of 200 µL TNP (1 mM).

Table S3. Comparison of K_{SV} values and quenching efficiencies for nitro-phenol derivatives in **1** and **2**.

Nitro-analyte	K_{SV} value in 1	K_{SV} value in 2	Quenching efficiency (%) in 1	Quenching efficiency (%) in 2
TNP	3.55 X 10^4	4.97 X 10^4	87	91
2,4-DNP	3.14 X 10^4	2.49 X 10^4	76	83
4-NP	1.90 X 10^4	2.02 X 10^4	71	74

Table S4. Literature survey on detection limit, K_{SV} and K_q values for TNP.

Organic Probe	K_{sv} (M^{-1})	K_q $M^{-1}s^{-1}$	Detection Limit	Solvent Medium	Reference
bqbpbn (**1**) bqbpxn (**2**)	3.55 x 10^4 4.97 x 10^4	6.56 x 10^{12} 9.84 x 10^{12}	5.17 x 10^{-6} M (1.2 ppm) 1.37 x 10^{-6} M (0.3 ppm)	H_2O H_2O	**This work** **This work**
banthbpbn bnaphbpbn	5.78 x 10^4 3.26 x 10^4	5.58 x 10^{12} 4.68 x 10^{12}	0.6 ppm 1.6 ppm	H_2O H_2O	*ACS Omega*, 2018, **3**, 3248–3256
DQB	NA	NA	1.5 x 10^{-6} M (0.34 ppm)	CH_3CN:H_2O (1:1, v/v)	*New J. Chem.*, 2018, **42**, 8408-8414
F1 F2	3.94 x 10^4 2.10 x 10^4	NA	5.7 x 10^{-7} M (0.13 ppm) 9.3 x 10^{-7} M (0.21 ppm)	H_2O H_2O	*Chem. Commun.*, 2017, **53**, 10524-10527
1-(3-chloropropyl)-3-((7-hydroxy-2-oxo-2H-chromen-4-yl)methyl)-1Hbenzo[d] imidazol-3-ium chloride	1.58 x 10^4	NA	2.08 x 10^{-7} M	H_2O	*ChemistrySelect*, 2016, **1**, 1756-1762
DBSA-PANI	16.8 x 10^6	NA	1 x 10^{-6} M	NMP	*ChemistrySelect*, 2018, **3**, 2655-2664
Compound 1	3.43 x 10^3	NA	15.2 x 10^{-6} M (3.48 ppm)	H_2O	*Cryst. Growth Des.*, 2015, **15**, 3493-3497
PA PF	1.77 x 10^4 3.90 x 10^4	NA NA	NA NA	H_2O	*Sensors and Actuators, B* 2014, **203**, 612-620
PrPr	10^5	NA	13 μM (2.98 ppm)	CH_3CN	*CrystEnggComm*, 2017, **19**, 6703-6710
R1	4.37 x 10^4	NA	0.0032 μM (0.73 ppb)	DMSO:H_2O (1:4)	*ACS Omega*, 2017, **2**, 1583–1593
Nph-An	7.0 x 10^4	NA	4.7 x 10^{-7} M (0.11 ppm)	THF:H_2O (1:9)	*Sensors and Actuators, B* 2016, **230**, 746-752
Amphiphile 1	NA	NA	1.55 x 10^{-7} M (0.035 ppm)	EtOH:H_2O (2:3)	*ACS Omega*, 2016, **1**, 371–377
DNSA-SQ	NA	NA	7 x 10^{-8} M (0.016 ppm)	CH_3CN:H_2O (9:1)	*Chem. Commun.*, 2013, **49**, 4764-4766
P3 P4	2.69 x 10^4 8.08 x 10^4	NA NA	31-70 ppm	$CHCl_3$	*J. Mater. Chem. C*, 2017, **5**, 11100-11110
L	NA	NA	4.3 x 10^{-7} M (0.098 ppm)	DMF	*Chem. Commun.*, 2011, **47**, 4505-4507
Cage 4	2.2 x 10^5	NA	6.4 ppb	DCM	*Chem. Commun.*, 2014, **50**, 15788-15791

Table S5. HOMO and LUMO energies calculated for **1**, **2** and NACs using DFT with basis set B3LYP/6- 31G+(dp) and Gaussian09 program.

	HOMO (eV)	LUMO (eV)	Band Gap (eV)
1	-6.0360	-1.7140	4.322
2	-5.9492	-1.9631	3.9861
TNP	-8.2374	-3.8978	4.3396
2,4-DNP	-7.6644	-2.8202	4.8442
4-NP	-6.9207	-2.2213	4.6994
TNT	-8.4592	-3.4926	4.9666
2,4-DNT	-7.7645	-3.2174	4.5471
2,6-DNT	-7.6448	-3.2877	4.3571
1,3-DNB	-7.9855	-3.4311	4.5544
NB	-7.5912	-2.4283	5.1629

Table S6. Average lifetimes of **1** and **2** before and after TNP addition.

	1	**1 +** 20 μL **TNP**	**1 +** 40 μL **TNP**	**1 +** 200 μL **TNP**	**2**	**2 +** 20 μL **TNP**	**2 +** 40 μL **TNP**	**2 +** 200 μL **TNP**
χ^2 value	1.10	1.18	1.16	1.14	1.17	1.19	1.10	1.13
τ_1 (ns)	0.34	0.37	0.28	0.20	1.33	1.25	1.29	1.19
α_1	0.392	0.416	0.386	0.346	0.245	0.135	0.163	0.278
τ_2 (ns)	1.72	1.96	1.81	1.50	0.15	0.09	0.113	0.093
α_2	0.493	0.498	0.512	0.499	0.663	0.801	0.772	0.671
τ_3 (ns)	9.07	9.96	7.63	5.16	7.52	6.72	6.75	1.19
α_3	0.114	0.085	0.100	0.153	0.091	0.063	0.064	0.278
Average τ (ns)	**5.41**	**5.28**	**4.19**	**3.02**	**5.06**	**4.60**	**4.38**	**3.29**